A Quantile Approach to Evaluating Asset Pricing Models

Tjeerd de Vries *

This Version: February 19, 2023
First draft: June 2021

Abstract

This paper studies the misspecification of asset pricing models by examining the local difference between the physical and risk-neutral measure. Using quantile regression, I find that the conditional physical distribution differs most from the risk-neutral distribution in the left tail, while the right tails of both distributions are almost identical. I propose a new bound on the volatility of the stochastic discount factor (SDF) to show that the local difference in the left tail implies that the SDF is highly volatile. Finally, I propose a lower bound on the difference between the physical and risk-neutral distribution in the left tail, which is approximately tight in the data. I interpret the bound as a real time measure of the Peso problem and find that it fluctuates significantly over time. At the height of the 2008 financial crisis and 2020 Covid crisis, the bound predicts that a market return of -28% or lower has a 5% probability. Both findings provide evidence for time varying disaster risk.

Keywords: Asset pricing, Model misspecification, Quantile methods

JEL Codes: G13, G17, C14, C22

*Department of Economics, University of California San Diego. Email: tjdevrie@ucsd.edu. I would like to thank Alexis Toda, Allan Timmermann, James Hamilton, Xinwei Ma, Yixiao Sun, Rossen Valkanov, Brendan Beare, Caio Almeida and participants of the 2022 SoFiE conference for useful feedback. All errors are my own.

1 Introduction

Asset pricing models are essential tools for understanding the dynamics of financial markets and predicting the behavior of asset prices. Evaluating the misspecification of these models is crucial for understanding why a particular modeling approach falls short in explaining certain characteristics of the data. For example, Hansen and Jagannathan (1991) (HJ henceforth) show that the Sharpe ratio puts a tight constraint on the volatility of the stochastic discount factor, which can be used to sieve out potential asset pricing models.

In this paper, I propose a new way to analyze model misspecification in asset pricing based on *local differences* between the physical and risk-neutral distribution. The basic insight is that any statistic of interest, such as the equity or variance premium, is determined by differences between the physical and risk-neutral distribution. I use quantiles to locally measure the difference between these distributions which allows me to dissect what part of a model's return distribution is most misspecified. This approach contrasts with previous literature that relies on global information bounds such as the Sharpe ratio, which aggregate information from the return distribution.

I start by providing empirical evidence that the conditional physical and risk-neutral distribution of the S&P500 index differ most in the left tail. We cannot directly measure this difference since the physical distribution is unobserved, even though the risk-neutral distribution can be identified from option prices (Breeden and Litzenberger, 1978). To proceed, I use quantile regression (QR) to estimate

$$\underbrace{Q_{t,\tau}(R_{m,t\to N})}_{\text{Unobserved}} = \beta_0(\tau) + \beta_1(\tau)\underbrace{\widetilde{Q}_{t,\tau}(R_{m,t\to N})}_{\text{Observed}} \qquad \tau \in (0,1), \tag{1.1}$$

where $Q_{t,\tau}$, $\widetilde{Q}_{t,\tau}$ denote the physical and risk-neutral quantile respectively of the market return $R_{m,t\to N}$ at time t. The parameters in (1.1) can be estimated from a quantile regression of $R_{m,t\to N}$ on $\widetilde{Q}_{t,\tau}(R_{m,t\to N})$, since the realized market return is drawn from the physical distribution. Any deviation from the risk-neutral benchmark, $[\beta_0(\tau), \beta_1(\tau)] = [0, 1]$, signifies a local difference between the physical and risk-neutral measure at the τ-percentile. From the QR estimates, I find that (i) the risk-neutral benchmark cannot be rejected in the right tail (τ close to 1) but is decisively rejected in the left tail (τ close to 0); (ii) The explanatory power in- and out-of-sample is much higher in the right tail compared to the left tail. Hence, in order for an asset pricing model to be consistent with empirical data, it must produce a right tail of the physical distribution that is close to risk-neutral, since investors only get compensated for bearing downside risk. This feature is embedded in dis-

aster risk models, but cannot be achieved by models which assume that the market return follows a lognormal distribution. As byproduct of the QR estimates, I also provide new evidence that the pricing kernel is non-monotonic, without estimating the pricing kernel itself.

To understand the influence of local differences between the physical and risk-neutral measure on the pricing kernel, I introduce a *local bound* on the SDF volatility that is closely related to the HJ bound. The local bound depends on the following measure of dispersion:

$$\tau - \phi(\tau), \quad \tau \in (0,1),$$

where $\phi(\tau) = F(\widetilde{Q}_\tau(R))$ and $F(\cdot)$, $\widetilde{Q}_\tau(\cdot)$ denote the unconditional physical CDF and risk-neutral quantile of a generic return R. The quantity $\phi(\tau)$ is referred to as the *ordinal dominance curve* (ODC) of the physical and risk-neutral measure, and $\tau - \phi(\tau)$ can be thought of as a functional analogue of the equity premium. The local bound shows how any pointwise difference between the physical and risk-neutral measure leads to a volatile SDF. In the data, the local bound peaks around the 5^{th} percentile, which implies an SDF volatility of at least 30%. In contrast, the Sharpe ratio renders a much looser bound on the SDF volatility, of about 13%. I interpret this finding as favorable evidence for models that embed disaster risk, since these models imply that the physical and risk-neutral distribution locally differ most in the left tail. A global bound such as the Sharpe ratio does not reveal this local dispersion.

Based on my empirical findings that the physical and risk-neutral measures differ the most in the left tail, I propose a method for measuring this difference using a risk-adjustment term observed from option prices. This approach provides a model-free way to assess whether disaster risk changes over time. Using some elementary results from functional analysis, I show that up to first-order, the difference between the physical and risk-neutral quantile is directly proportional to $\tau - \phi_t(\tau)$, where $\phi_t(\tau)$ denotes the conditional ODC. Under mild economic constraints: $\tau - \phi_t(\tau) \geq \text{LB}_{t,\tau}$, where $\text{LB}_{t,\tau}$ can be computed from option prices. This result is reminiscent of the lower bounds on the equity premium of Martin (2017) and Chabi-Yo and Loudis (2020). Using quantile regression, I show that the risk-adjustment term captures most of the (unobserved) wedge between the physical and risk-neutral quantile function. Since the left tail of the physical quantile function is a good measure of disaster risk, I obtain a market observed proxy for disaster risk. In the data, this disaster risk proxy correlates well with events associated to high market uncertainty such as the 2008 financial crisis or the 2020 Covid pandemic. During these periods' peak, my measure predicts that with 5% probability, the (monthly) market return would drop by 28% or more. This probability is 57 times higher than historical data suggest.

Additionally, I find that the disaster risk measure fluctuates significantly over time, which is model-free evidence of time varying disaster risk.

I conclude by proposing several out-of-sample exercises to test the robustness of my findings. The literature on predicting excess returns highlights the importance of out-of-sample performance (Campbell and Thompson, 2008; Welch and Goyal, 2008), but many of the performance measures, such as the out-of-sample R^2, are tailored to OLS and cannot be applied to quantile regression. To address this issue, I propose a clean substitute for the out-of-sample R^2 in the context of quantile regression. Using this measure, I find that the risk-adjustment term better predicts the physical quantile than competing benchmarks. Unlike the equity premium, there is fewer guidance in the literature on variables that should predict quantiles. As a natural benchmark, I consider the VIX index since it is available daily and known to be correlated with negative market sentiment (Bekaert and Hoerova, 2014). Surprisingly, I find that the risk-adjustment term outperforms the VIX predictor in the left tail, even though the VIX uses in-sample information. This fact strengthens our interpretation of the risk-adjustment term as a measure of disaster risk since this term does not require any parameter estimation. Using the risk-neutral quantile as a predictor, I obtain the same result in the right tail of the return distribution.

Related literature. Our approach, which uses quantile regression to measure local dispersion between the physical and risk-neutral distribution, is related to a larger body of literature that estimates the pricing kernel from returns and option data (Aït-Sahalia and Lo, 2000; Jackwerth, 2000; Rosenberg and Engle, 2002; Beare and Schmidt, 2016; Cuesdeanu and Jackwerth, 2018). However, estimating the pricing kernel from returns and options can be challenging, especially in the tails of the distribution, where the ratio of densities that defines the pricing kernel can become unstable. In addition, using historical returns to estimate the physical density can lead to inconsistent results (Linn et al., 2018). In contrast, QR can be used to draw inference on the pricing kernel indirectly, by leveraging on the *observed* realized return and risk-neutral distribution, which avoids the estimation of a density ratio. Bakshi et al. (2010) use a somewhat similar idea to show that the pricing kernel is U-shaped.

Using the difference between the physical and risk-neutral distribution to screen asset pricing models starts with Hansen and Jagannathan (1991), who derived a nonparametric bound on the SDF volatility and used it to establish a duality relation with the maximum Sharpe ratio. Many researchers followed up with higher-order

moment bounds (Snow, 1991; Almeida and Garcia, 2012; Liu, 2021) and entropy bounds (Stutzer, 1995; Bansal and Lehmann, 1997; Alvarez and Jermann, 2005; Backus et al., 2014). These bounds all give some measure on how much the risk-neutral distribution differs from the physical distribution. All these measures are global, in that they use an average over the entire state space. The local volatility bound in this paper is a function, instead of a single statistic, and can be considered an intermediate case between a single bound and a full estimate of the SDF.

This paper is also related to the growing literature on using options to estimate forward-looking equity premiums (Martin, 2017; Martin and Wagner, 2019; Chabi-Yo and Loudis, 2020). However, unlike those papers that focus on the conditional expectation of excess returns, this paper uses option data to predict conditional return quantiles. The relationship between option prices and expected market return shocks has been extensively studied in the literature (Bates, 1991, 2000, 2008; Coval and Shumway, 2001; Bollerslev and Todorov, 2011; Backus et al., 2011; Ross, 2015). Similar to Bollerslev and Todorov (2011), this paper obtains a nonparametric measure of fear or disaster risk. However, the approach differs in that it only uses risk-neutral information and is motivated by the interplay between the physical and risk-neutral quantile function. This approach also complements the recovery literature (Ross, 2015; Borovička et al., 2016; Qin and Linetsky, 2017) as it derives forward-looking approximations to the left and right tail of the physical distribution using option data. The time variation in the approximation for the left tail quantile documented in this paper is consistent with the time-varying disaster risk models of Gabaix (2012) and Wachter (2013).

The QR approach used in this paper is similar to conditional mean regressions that are common in the equity premium literature. The performance evaluation of conditional expected return predictors is well established in the literature, with seminal contributions from Campbell and Thompson (2008) and Welch and Goyal (2008). To evaluate the performance of the QR approach, I draw on earlier work by Koenker and Machado (1999) and extend the evaluation toolkit to the quantile setting, specifically focusing on out-of-sample performance. This paper thus complements the literature on conditional return prediction by extending it to the entire distribution.

The rest of this paper is organized as follows. Section 2 gives a preview of the physical and risk-neutral distribution in two common asset pricing models. Section 3 fixes notation and presents the main empirical results from the QR regressions. Section 4 introduces the local bound and discusses its use in asset pricing models,

and Section 5 estimates the local bound with actual data. Section 6 complements the results from Section 2 and shows how risk-neutral information can be used to measure disaster risk. Finally, Section 7 concludes.

2 Physical and Risk-Neutral Distribution in two Leading Asset Pricing Models

Asset pricing models can be differentiated based on the drivers as well as statistical properties of the SDF. Once we fix the physical distribution, changes in the SDF translate into changes in the risk-neutral distribution and vice versa. To gain intuition for our approach, Figure 1 shows the physical and risk-neutral distribution in two leading asset pricing models, namely the long-run risk model of Bansal et al. (2012) and the disaster risk model of Rietz (1988) and Barro (2006).[1] Both models are successful in explaining a high equity premium, but from Figure 1 it is clear that both models have rather different predictions about the local difference between the physical and risk-neutral measure.

First, the disaster risk model in panel 1a shows that the difference between the two distributions is most pronounced in the left tail, whereas the long-run risk (LRR) model in panel 1b predicts that the difference is negligible in that region. The tails of both distributions in the LRR model are similar because of the conditional lognormal assumption, whereas the left tails in the disaster risk model are rather different due to jump risk. Second, the disaster risk model implies that the physical and risk-neutral distribution are almost identical beyond the median, since upside does not carry a risk premium. We cannot directly test which model is more in line with the data, since the conditional physical distribution is unobserved. Nevertheless, in the next Section I show that we don't need to estimate the physical distribution to test a model's prediction about the local difference between the physical and risk-neutral distribution.

3 Main Empirical Results

This section documents QR estimates of the realized return on the risk-neutral quantile function to study the local difference between the physical and risk-neutral distribution. Before presenting the results, I first discuss the notation used in this section.

[1] I discuss these models, as well as their calibration in more detail in Section 4.2.

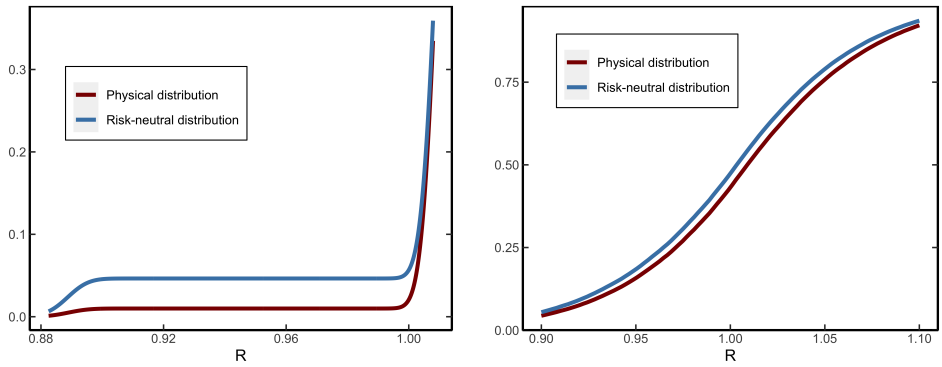

(a) Disaster risk

(b) Long-run risk

Figure 1: **Physical and risk-neutral distribution in the disaster risk and long-run risk model.** Panels (a) and (b) show the physical and risk-neutral distribution in the disaster risk and long-run risk model respectively. Both models are calibrated at a monthly frequency.

3.1 Notation

Let $R_{m,t\to N}$, denote the market return from period t to $t+N$, where N is typically 30, 60 or 90 days. The risk-free rate over the same period is denoted by $R_{f,t\to N}$, which is assumed to be known at time t. In the absence of arbitrage, there exists a positive random variable $M_{t\to N}$ such that, conditional on all time t information

$$\mathbb{E}_t\left[M_{t\to N}R_{m,t\to N}\right]=1. \tag{3.1}$$

The random variable $M_{t\to N}$ is referred to as the stochastic discount factor (SDF) and the expectation in (3.1) is calculated under the *physical* probability measure $\mathbb{P}_t$, which is the actual distribution of the market return. The SDF can potentially depend on many state variables. To avoid having to specify or estimate these state variables, I work with the projected SDF

$$M_{t\to N}=\mathbb{E}_t\left[M^*_{t\to N}|R_{m,t\to N}\right],$$

where $M^*_{t\to N}$ is the SDF that depends on all the state variables. The projected SDF has the same pricing implications for contingent claims written on the observed return (Cochrane, 2005, pp. 66–67). It is convenient to restate (3.1) in terms of risk-neutral probabilities:

$$\widetilde{\mathbb{E}}_t\left(R_{m,t\to N}\right)=1/\mathbb{E}_t\left[M_{t\to N}\right]=R_{f,t\to N},$$

where the expectation is calculated under the risk-neutral measure $\widetilde{\mathbb{P}}_t$.[2] Finally, $F_t(x) \coloneqq \mathbb{P}_t(R_{m,t\to N} \leq x)$ denotes the physical CDF of the market return conditional on all information available at time t, $f_t(\cdot)$ denotes the conditional PDF and $Q_{t,\tau}$ denotes the conditional τ-quantile. As before, a tilde superscript refers to the risk-neutral measure, so that

$$\widetilde{F}_t(\widetilde{Q}_{t,\tau}) = \widetilde{\mathbb{P}}_t\left(R_{m,t\to N} \leq \widetilde{Q}_{t,\tau}\right) = \tau, \qquad \text{for } \tau \in (0,1).$$

The physical and risk-neutral quantile depend on the underlying random variable $R_{m,t\to N}$ (i.e. $\widetilde{Q}_{t,\tau} \coloneqq \widetilde{Q}_{t,\tau}(R_{m,t\to N})$), but I typically omit this dependence as the underlying random variable should be clear from the context.

3.2 Data

I need data on the market return and the risk-neutral distribution over time to estimate the quantile regressions in the next section. The market return gives information about the conditional physical distribution, since the distribution of $R_{m,t\to N}$ is $\mathbb{P}_t$, conditional on time t. I use *overlapping returns* on the S&P500 index from WRDS over the period 2003–2021 to represent the market return. Second, I use put and call option prices on the S&P500 on each day t from OptionMetrics to estimate the risk-neutral quantile function $\widetilde{Q}_{t,\tau}$ nonparametrically based on the Breeden and Litzenberger (1978) formula:

$$\widetilde{F}_t\left(\frac{K}{S_t}\right) = R_{f,t\to N}\frac{\partial}{\partial K}\text{Put}_t(K), \tag{3.2}$$

where $\text{Put}_t(K)$ denotes the time t price of a European put option on the S&P500 with price S_t, strike price K and expiration date $t+N$. It is a nontrivial exercise to obtain solid estimates of $\widetilde{F}_t$ (and hence $\widetilde{Q}_{t,\tau}$) from (3.2) due to the lack of a continuum of option prices, interpolation of different maturity options and missing data for option prices far in– and out-of-the money. A detailed description of my approach that overcomes these issues is described in Appendix B.2, which is based on Filipović et al. (2013).[3] Finally, I obtain the risk-free rate from Kenneth French's website.[4]

[2] The second equality above is valid whenever the risk-free rate exists, which I assume throughout this Section.

[3] This approach uses a kernel density and adds several correction terms to approximate the risk-neutral density. I follow Barletta and Santucci de Magistris (2018) and use a principal components step to avoid overfitting in the tails.

[4] See http://mba.tuck.dartmouth.edu/pages/faculty/ken.french/data_library.html#Research

3.3 Risk-neutral quantile regression

In principle, if we observe the conditional phyisical and risk-neutral distribution, we can use it to test almost any prediction that a model makes about the market return.[5] Unfortunately, the physical distribution cannot be recovered in a model-free way from option prices, unless one makes strong assumptions about the martingale component of the SDF (Ross, 2015; Borovička et al., 2016).[6]

I use an indirect approach to gauge which part of the physical distribution differs from the risk-neutral distribution. Suppose momentarily that the physical quantile is given by

$$Q_{t,\tau}(R_{m,t\to N}) = \beta_0(\tau) + \beta_1(\tau)\widetilde{Q}_{t,\tau}(R_{m,t\to N}), \qquad \forall \tau \in (0,1). \tag{3.3}$$

Given a sample of T observations $\{R_{m,t\to N}, \widetilde{Q}_{t,\tau}\}_{t=1}^{T}$, we can estimate the unknown parameters using quantile regression (Koenker and Bassett, 1978):

$$[\widehat{\beta}_0(\tau), \widehat{\beta}_1(\tau)] = \underset{\beta_0,\beta_1\in\mathbb{R}}{\arg\min} \sum_{t=1}^{T} \rho_\tau(R_{m,t\to N} - \beta_0 - \beta_1\widetilde{Q}_{t,\tau}), \tag{3.4}$$

where $\rho_\tau(x) = x(\tau - \mathbb{1}(x < 0))$ is the check function from QR. Even if (3.3) is misspecified, Angrist et al. (2006) show that QR finds the best linear approximation to the conditional quantile function.[7] The use of QR to estimate the difference between the physical and risk-neutral distribution is rather different from common approaches in the literature that estimate the SDF using a physical PDF from historical data (see, for example, Aït-Sahalia and Lo (2000), Jackwerth (2000) and Rosenberg and Engle (2002)). The QR approach leverages on directly observed data $\{R_{m,t\to N}, \widetilde{Q}_{t,\tau}\}_{t=1}^{T}$ that also belong to the same information set. Hence, this approach is not prone to the mismatched information critique of Linn et al. (2018).

If the world is risk-neutral, $Q_{t,\tau}(R_{m,t\to N}) = \widetilde{Q}_{t,\tau}$ and $[\widehat{\beta}_0(\tau), \widehat{\beta}_1(\tau)] \to [0,1]$ in probability. More generally, the disaster risk model predicts $[\beta_0(\tau), \beta_1(\tau)] \approx [0,1]$ for all $\tau > \kappa > 0.5$, for some κ far enough in the right tail. QR allows me to assess these different hypotheses by testing how close $[\beta_0(\tau), \beta_1(\tau)]$ is to the $[0,1]$ benchmark for different τ. The setup in (3.3) is nonstandard since the regressor changes with τ, unlike most quantile regressions where the independent variable is fixed across τ.

[5] For example, the equity premium can be expressed as: $\mathbb{E}_t\left[R_{m,t\to N}\right] - R_{f,t\to N} = \int x \,\mathrm{d}(F_t - \widetilde{F}_t)(x)$. Similarly, any other statistic of the market return is a functional of the physical and risk-neutral distribution.

[6] This impossibility result contrasts with (3.2), which shows that the risk-neutral distribution can be recovered nonparametrically from option prices.

[7] This result is analogous to OLS, which finds the best linear approximation to the conditional *expectation* function, even if the model is misspecified.

Table 1 shows the QR estimates of (3.4). The null hypothesis that $[\beta_0(\tau), \beta_1(\tau)] = [0, 1]$ is (borderline) rejected for all $\tau \leq 0.2$, at all horizons. In contrast, the null hypothesis is never rejected for $\tau \geq 0.8$ and the point estimates are close to $[0, 1]$ at all horizons. These results suggest that the physical and risk-neutral distribution locally differ most in the left tail conditional on time t, exactly as the disaster risk model predicts. The standard errors in Table 1 are obtained by the smooth extended tapered block bootstrap (SETBB) of Gregory et al. (2018), which is robust to heteroscedasticity and weak dependence. This robustness is important in the estimation, since I use overlapping returns which creates time dependence in the error term, akin to the overlapping observation problem in OLS (Hansen and Hodrick, 1980). SETBB also renders an estimate of the covariance matrix between $\widehat{\beta}_0(\tau)$ and $\widehat{\beta}_1(\tau)$, which can be used to test joint restrictions on the coefficients.[8]

Table 1 contains two other measures of fit that can be used measure how well the risk-neutral distribution approximates the physical distribution. The first measure, $R^1(\tau)$, is defined as[9]

$$R^1(\tau) \coloneqq 1 - \frac{\min_{b_0,b_1} \sum_{t=1}^{T} \rho_\tau(R_{m,t\to N} - b_0 - b_1 \widetilde{Q}_{t,\tau})}{\min_{b_0} \sum_{t=1}^{T} \rho_\tau(R_{m,t\to N} - b_0)}. \tag{3.5}$$

This measure of fit was proposed by Koenker and Machado (1999) and is a clean substitute for the OLS R^2. Table 1 shows that the in-sample fit in the right tail is much better compared to the left tail according to $R^1(\tau)$. Second, to measure the out-of-sample fit, I use

$$R^1_{oos}(\tau) \coloneqq 1 - \frac{\sum_{t=w}^{T} \rho_\tau(R_{m,t\to N} - \widetilde{Q}_{t,\tau})}{\sum_{t=w}^{T} \rho_\tau(R_{m,t\to N} - \overline{Q}_{t,\tau})}, \tag{3.6}$$

where $\overline{Q}_{t,\tau}$ is the *historical rolling quantile* of the market return from time $t-w+1$ to t and w is the rolling window length. $R^1_{oos}(\tau)$ is a natural analogue of the out-of-sample R^2 proposed by Campbell and Thompson (2008) in the context of conditional mean regression. Notice that (3.6) is a genuine out-of-sample metric, since no parameter estimation is used. Table 1 shows that, out-of-sample, the risk-neutral quantile fares better in the right tail than in the left tail. Hence, the risk-neutral distribution approximates the physical distribution much better in the right tail, both in- and out-of-sample. Investors in the market return thus get compensated for bearing downside risk, but not upside risk. These findings provide support for the assump-

[8] I use the `QregBB` function from the *R* package `QregBB`, available on the author's Github page: https://rdrr.io/github/gregorkb/QregBB/man/QregBB.html. The only user required input for this method is the block length in the bootstrap procedure.

[9] It is well known that b_0 in the denominator of (3.5) equals the in-sample τ-quantile.

Table 1: **Risk-neutral quantile regression**

Horizon	τ	$\widehat{\beta}_0(\tau)$	$\widehat{\beta}_1(\tau)$	Wald test	Hit[%]	$R^1(\tau)$[%]	$R^1_{oos}(\tau)$[%]
30 days*	0.05	0.43 (0.225)	0.56 (0.240)	0.01	-2.67	6.28	6.11
	0.1	0.45 (0.241)	0.54 (0.251)	0.03	-3.56	3.45	1.01
	0.2	0.69 (0.399)	0.30 (0.407)	0.11	-3.73	0.55	0.89
	0.5	−0.60 (0.307)	1.61 (0.305)	0	-8.07	1.65	2.24
	0.8	−0.09 (0.160)	1.09 (0.156)	0.2	-3.24	12.44	12.5
	0.9	0.03 (0.123)	0.97 (0.118)	0.97	-0.04	20.41	21.88
*(Obs. 4333)	0.95	0.12 (0.122)	0.89 (0.116)	0.51	0.27	27.07	31.31
60 days**	0.05	0.45 (0.323)	0.54 (0.367)	0.01	-3.33	3.12	13.14
	0.1	0.58 (0.324)	0.41 (0.348)	0.02	-5.57	1.79	3.5
	0.2	0.78 (0.424)	0.21 (0.436)	0.05	-6.6	0.38	-0.03
	0.5	−1.02 (0.426)	2.01 (0.421)	0.02	-7.88	2.81	3.86
	0.8	−0.08 (0.209)	1.08 (0.120)	0.11	-5.53	12.7	12.23
	0.9	0.04 (0.149)	0.96 (0.141)	0.57	-1.94	21.66	22.79
**(Obs. 4312)	0.95	0.04 (0.130)	0.96 (0.121)	0.91	0.43	31.07	34.19
90 days***	0.05	0.60 (0.438)	0.37 (0.518)	0.02	-2.95	2.9	15.63
	0.1	0.59 (0.412)	0.40 (0.456)	0	-6.36	3.46	3.84
	0.2	0.57 (0.593)	0.43 (0.613)	0.09	-7.53	0.83	1.93
	0.5	−0.99 (0.653)	1.99 (0.641)	0.03	-10.85	2.58	0.18
	0.8	−0.23 (0.258)	1.23 (0.244)	0.32	-6.66	15.47	16.54
	0.9	−0.02 (0.184)	1.02 (0.170)	0.86	-1.12	23.18	27.92
***(Obs. 4291)	0.95	0.08 (0.158)	0.93 (0.144)	0.87	-0.06	32.14	39.88

Note: This table reports the QR estimates of (3.4) over the sample period 2003–2021 at different horizons, using overlapping returns. Standard errors are shown in parentheses and based on SETBB with a block length of 5 times the prediction horizon. *Hit* refers to the sample expectation of (3.7). $R^1(\tau)$ denotes the goodness of fit measure (3.5). $R^1_{oos}(\tau)$ is the out-of-sample goodness of fit (6.19) (based on $\widetilde{Q}_{t,\tau}$), using a rolling window of size 10 times the prediction horizon.

tion in (time varying) disaster risk models (Rietz, 1988; Barro, 2006; Gabaix, 2012; Wachter, 2013) that shocks to the market return are negative conditional on a disaster occurring.

Table 1 connects to other misspecification metrics previously investigated in the literature, such as monotonicity of the pricing kernel. The "Hit" column in Table 1

reports the expected value of:[10]

$$\text{Hit}_t = \mathbb{1}\left(R_{m,t\to N} < \widetilde{Q}_{t,\tau}\right) - \tau. \tag{3.7}$$

The expected value of Hit_t yields another measure of the difference between F_t and $\widetilde{F}_t$. In particular, the expected value is 0 if investors are risk-neutral. It turns out that (3.7) is negative for all τ if the pricing kernel is a monotonic function of $R_{m,t\to N}$.[11] Contradicting monotonicity, Table 1 shows that the sample expectation of Hit_t is positive for $\tau = 0.95$, at the 30 and 60 day horizon. I find, using stationary bootstrap, that the estimated expectation is significantly different from zero. This result is consistent with a U-shaped pricing kernel which has previously been documented in the literature (see Aït-Sahalia and Lo (1998), Jackwerth (2000), Rosenberg and Engle (2002), Bakshi et al. (2010), Beare and Schmidt (2016) and Cuesdeanu and Jackwerth (2018)).

Finally, Table 1 also connects to the recovery of beliefs (Ross, 2015; Borovička et al., 2016). Namely, the right tail of the physical distribution can be accurately recovered from the right tail of the risk-neutral distribution, which is observed conditional on time t. Hence, there is a specific part of the return distribution that can be recovered from option prices. In Section 6, I outline how we can approximately recover the left tail of the physical distribution.

3.4 Lognormal returns and risk-neutral quantiles

Using the risk-neutral quantile in QR as a regressor is new and nonstandard, as the regressor changes with τ. To provide additional motivation for including the risk-neutral quantile as a regressor, I show that the risk-neutral quantile is an optimal regressor if the return follows a lognormal distribution. I then verify that the risk-neutral quantile is not optimal in the data, which provides evidence against the conditional lognormal assumption.

To describe the environment, consider the following discretized version of the Black-Scholes model. There is a riskless asset that offers a certain return, $R_{f,t\to N} = e^{r_f N}$, and a risky asset with return $R_{m,t\to N} = \exp([\mu - \frac{1}{2}\sigma_t^2]N + \sigma_t\sqrt{N}Z_{t+N})$, where Z_{t+N} is standard normal, and σ_t is the conditional volatility of returns. In this setup, $M_{t\to N} \coloneqq \exp(-[r_f + \xi_t^2/2]N - \xi_t\sqrt{N}Z_{t+N})$ is a valid SDF with conditional Sharpe

[10] The Hit_t function was first introduced by Engle and Manganelli (2004).

[11] To see this, we can directly apply the arguments of Beare and Schmidt (2016), who show that monotonicity is equivalent to the ordinal dominance curve being concave (or convex, since we define the ordinal dominance curve as $\phi(\tau) = F(\widetilde{F}^{-1}(x))$).

ratio

$$\xi_t = \frac{\mu - r_f}{\sigma_t}.$$

The implied dynamics under risk-neutral measure are given by

$$R_{m,t\to N} = \exp\left((r_f - \frac{1}{2}\sigma_t^2)N + \sigma_t\sqrt{N}Z_{t+N}\right). \tag{3.8}$$

Proposition 3.1 shows that quantile regression of the risk-neutral quantile on the realized return renders an identical forecast when using the (unobserved) physical quantile as a regressor.

Proposition 3.1. *Consider the lognormal model described above with return observations* $\{R_{m,t\to N}\}_{t=1}^T$ *stacked in the* $T \times 1$ *vector* R*. Let* $\widetilde{X}_t(\tau) \coloneqq [1\ \widetilde{Q}_{t,\tau}(R_{m,t\to N})]$ *and denote the* $T\times 2$ *matrix of stacked* $\widetilde{X}_t(\tau)$ *by* $\widetilde{X}(\tau)$*. Define the regression quantile* $\widehat{\beta}(\tau; R, \widetilde{X}(\tau))$ *as the solution to the quantile regression with the risk-neutral quantile as regressor:*

$$\widehat{\beta}(\tau; R, \widetilde{X}(\tau)) = \underset{\beta\in\mathbb{R}^2}{\arg\min} \sum_{t=1}^T \rho_\tau\left(R_{m,t\to N} - \widetilde{X}_t(\tau)^\top\beta\right).$$

Similarly, let $X_t(\tau) \coloneqq [1\ Q_{t,\tau}(R_{m,t\to N})]$*,* $X(\tau)$ *denote the* $T\times 2$ *matrix of stacked* $X_t(\tau)$ *and define* $\widehat{\beta}(\tau; R, X(\tau))$ *as the solution to the quantile regression using the physical quantile as regressor:*

$$\widehat{\beta}(\tau; R, X(\tau)) = \underset{\beta\in\mathbb{R}^2}{\arg\min} \sum_{t=1}^T \rho_\tau\left(R_{m,t\to N} - X_t(\tau)^\top\beta\right). \tag{3.9}$$

Then,

$$\widetilde{X}_{T+1}(\tau)\widehat{\beta}(\tau; R, \widetilde{X}(\tau)) = X_{T+1}(\tau)\widehat{\beta}(\tau; R, X(\tau)). \tag{3.10}$$

Proof. See Appendix A.1. ■

In sum, if returns are conditionally lognormal with time varying volatility there is no need to risk adjust, since the quantile forecast based on the risk-neutral quantile satisfies

$$Q_{T+1,\tau}(R_{m,T+1\to N}) = \widetilde{Q}_{T+1,\tau}\widehat{\beta}_1(\tau) + o_p(1).$$

Intuitively, the reason is that $\widehat{\beta}_1(\tau)$ picks up the risk premium, so that $\widetilde{Q}_{t,\tau}\widehat{\beta}_1(\tau)$ rotates back into physical quantile units. A similar situation occurs in Principal Component Analysis, where it is enough to identify the principal component up to some rotation matrix to make predictions (Bai, 2003). Proposition 3.1 hinges on the assumption that changes in conditional volatility are the only source of time variation in the distribution of returns.

Proposition 3.1 can be used as model free evidence against the conditional lognormal assumption. To see this, we can use QR based on the first t_0 observations to estimate the model

$$Q_{t,\tau}(R_{m,t\to N}) = \widehat{\beta}_{0,t_0}(\tau) + \widehat{\beta}_{1,t_0}(\tau)\widetilde{Q}_{t,\tau}, \tag{3.11}$$

where the t_0-subscript in $\beta_{\cdot,t_0}$ refers to the fact that the coefficients are estimated using observations up to time t_0. I use an expanding window to estimate $\beta_{\cdot,t_0}$ in (3.11), which are used to produce dynamic quantile forecasts of the form

$$\widehat{Q}^{\text{logn}}_{t,\tau} = \widehat{\beta}_{0,t}(\tau) + \widehat{\beta}_{1,t}(\tau)\widetilde{Q}_{t,\tau}. \tag{3.12}$$

If returns follow the lognormal dynamics in (3.8), Proposition 3.1 suggests that

$$Q_{t,\tau}(R_{m,t\to N}) \approx \widehat{Q}^{\text{logn}}_{t,\tau}.$$

This approximation can be formalized by testing the joint restriction

$$H_0: \quad [\beta_0(\tau), \beta_1(\tau)] = [0,1]^\top, \tag{3.13}$$

in the quantile regression

$$\min_{\beta_0,\beta_1\in\mathbb{R}} \sum_t \rho_\tau \left(R_{m,t\to N} - \beta_0 - \beta_1 \widehat{Q}^{\text{logn}}_{t,\tau} \right).$$

The results are summarized in Table 2. The point estimates are quite far from the $[0,1]^\top$ benchmark. The Wald test on the joint restriction is rejected for $\tau \in \{0.05, 0.1\}$, but fails to reject for $\tau = 0.2$ at both prediction horizons. Additionally, the explanatory power is low relative to Table 5, as can be seen from the $R^1(\tau)$ statistic. These numbers provide strong evidence against the conditional lognormal assumption, which is in line with our results from Section 3.3 and evidence from the literature (see e.g. Martin (2017, Result 4)).

4 Local bound on the SDF volatility and model implications

4.1 Local bound

The previous section showed that the physical and risk-neutral distribution locally differ most in the left tail. In this section, I show that these local differences imply that the SDF must be highly volatile; an observation that is closely related to the

Table 2: **Expanding quantile prediction with risk-neutral quantile**

	Horizon (in days)	$\widehat{\beta}_0(\tau)$	$\widehat{\beta}_1(\tau)$	Wald test	$R^1(\tau)$[%]	Obs
$\tau = 0.05$	30	0.54 (0.186)	0.42 (0.194)	0	4.36	3804
	60	0.55 (0.293)	0.39 (0.314)	0.11	1.84	3753
	90	0.78 (0.335)	0.11 (0.353)	0.01	0.88	3702
$\tau = 0.1$	30	0.59 (0.233)	0.39 (0.240)	0.03	2.39	3804
	60	0.80 (0.382)	0.16 (0.397)	0.06	0.22	3753
	90	0.74 (0.416)	0.21 (0.433)	0.09	1.34	3702
$\tau = 0.2$	30	0.83 (0.422)	0.15 (0.429)	0.14	0.28	3804
	60	0.87 (0.508)	0.11 (0.517)	0.23	0.25	3753
	90	0.73 (0.528)	0.26 (0.534)	0.37	0.52	3702

Note: This table reports the QR estimates of (3.12) using an expanding window based on an initial 500 observations. The sample period is 2003-2021. *Wald test* denotes the p-value of the joint restriction $[\beta_0(\tau), \beta_1(\tau)]^\top = [0, 1]^\top$. Standard errors are reported in parentheses and calculated using the SETBB with a block length of 5 times the prediction horizon. $R^1(\tau)$ denotes the goodness of fit measure (3.5).

Hansen and Jagannathan (1991) bound.

Since this section deals with unconditional distributions, I omit the t subscript from the notation and write R to denote a generic return. For ease of notation, I also define $\phi(\tau) \coloneqq F(\widetilde{Q}_\tau(R))$, which can be interpreted as the ordinal dominance curve of the measures $\mathbb{P}$ and $\widetilde{\mathbb{P}}$ (Hsieh and Turnbull, 1996). Finally, let $\aleph^+ := \{M : M \geq 0 \text{ and } \mathbb{E}(MR) = 1\}$, the space of all nonnegative SDFs (Hansen and Jagannathan, 1991). The volatility bound on the SDF can now be stated as follows.

Theorem 4.1 (Local volatility bound)**.** *Assume no-arbitrage, then for any $M \in \aleph^+$, we have*

$$\frac{\sigma(M)}{\mathbb{E}[M]} \geq \frac{|\tau - \phi(\tau)|}{\sqrt{\phi(\tau)(1-\phi(\tau))}} \qquad \forall \tau \in (0,1). \tag{4.1}$$

If a risk-free asset exists, then $\mathbb{E}[M] = 1/R_f$ and (4.1) simplifies to

$$\sigma(M) \geq \frac{|\tau - \phi(\tau)|}{\sqrt{\phi(\tau)(1-\phi(\tau))}R_f} \qquad \forall \tau \in (0,1). \tag{4.2}$$

Proof. See Appendix A.2. ■

If $\mathbb{P} = \widetilde{\mathbb{P}}$, agents are risk-neutral and the dominance curve evaluates to $\phi(\tau) = \tau$. In that case the local bound degenerates to zero. Theorem 4.1 makes precise the sense in which any local difference between the physical and risk-neutral distribution leads to a volatile SDF. Compare this to the classical HJ bound:

$$\sigma(M) \geq \frac{|\mathbb{E}(R) - R_f|}{\sigma(R) R_f}. \tag{4.3}$$

The lower bound in (4.3) shows that any excess return leads to a volatile SDF. Essentially, (4.3) uses three sources of information: (i) The mean of the physical distribution (ii) The mean of the risk-neutral distribution (iii) The variance of the physical distribution. The lower bound in (4.3) is also a global measure of distance between $\mathbb{P}$ and $\widetilde{\mathbb{P}}$, since the mean and volatility are averages across the whole distribution.

In contrast, the bound in (4.1) compares the physical and risk-neutral distribution for every τ-quantile, which is a *local* measure of distance between $\mathbb{P}$ and $\widetilde{\mathbb{P}}$. To clarify this local interpretation, I use a classical result of Hoeffding (see Appendix A.3):

$$\mathbb{COV}[R, M] = -\int_{-\infty}^{\infty} \mathbb{COV}[\mathbb{1}\left(R \leq x\right), M] \, \mathrm{d}x. \tag{4.4}$$

Equation (4.4) shows that $\mathbb{COV}[\mathbb{1}\left(R \leq x\right), M]$ locally measures the dependence between the SDF and return. The average over all local measures is equal to the global measure of dependence given by $\mathbb{COV}[R, M]$. HJ apply the Cauchy-Schwarz inequality to $\mathbb{COV}[R, M]$, in order to derive their bound on the SDF volatility. In contrast, I apply Cauchy-Schwarz to the local measure of dependence, $\mathbb{COV}[\mathbb{1}(R \leq \widetilde{Q}_\tau), M]$. This local measure is expected to yield sharper bounds on the SDF volatility if, for example, there is high tail dependence between the SDF and return.[12]

If there is no priced jump or stochastic volatility risk, $\phi(\tau)$ is determined by the equity premium and the HJ bound in (4.3) captures all relevant information. On the other hand, if there are risk premia for jumps or stochastic volatility, the measures $\mathbb{P}$ and $\widetilde{\mathbb{P}}$ differ both in shape and location (Broadie et al., 2009), which implies that $\phi(\tau)$ contains information that is not captured by the HJ bound. Moreover, the local bound is robust to fat-tails, since it is well defined regardless of any moment restrictions on the returns. Fat-tails and other higher order shape restrictions such as negative skewness are essential features of financial return data (see, e.g. Gao and Martin (2021)).

[12] See McNeil et al. (2015, Chapter 7.2.4) for a formal definition of tail dependence.

4.2 Local volatility and HJ bound in asset pricing models

In this section, I discuss the local volatility and HJ bound in (common) asset pricing models. These models make different predictions about the shape and strength of the local bound relative to the HJ bound. As such, the local bound can be used o diagnose potential model misspecification.

Example 4.1 (CAPM)**.** The Capital Asset Pricing Model (CAPM) specifies the SDF as

$$M = \alpha - \beta R_m.$$

Here, R_m denotes the return on the market portfolio. In this case $M \notin \aleph^+$, since the SDF can become negative. However, this probability is very small over short time horizons or we can think of M as an approximation to $M^* \coloneqq \max(0, M) \in \aleph^+$. Since the HJ bound is derived by applying the Cauchy-Schwarz inequality to $\mathbb{COV}(R_m, M)$, the inequality binds if M is a linear combination of R_m. Hence, under CAPM, the HJ bound is strictly stronger than the local bound regardless of the distribution of R_m.

Example 4.2 (Joint normality)**.** Suppose that M and R are jointly normally distributed and denote the mean and variance of R by μ_R and σ_R^2 respectively. The normality assumption violates no-arbitrage since M can be negative, but could be defended as an approximation over short time horizons when the variance is small (see Example 4.3). In Appendix A.3, I prove that

$$\left|\mathbb{COV}\left(\mathbb{1}\left(R \leq \widetilde{Q}_\tau\right), M\right)\right| = f_R(\widetilde{Q}_\tau)\left|\mathbb{COV}(R, M)\right|, \tag{4.5}$$

where $f_R(\cdot)$ is the marginal density of R.[13] This identity gives an explicit expression for the weighting factor in Hoeffding's identity (4.4). In Appendix A.3, I also derive an explicit expression for the relative efficiency between the local and HJ bound

$$\frac{\text{HJ bound}}{\text{local bound}} = \frac{\sqrt{\phi(\tau)(1-\phi(\tau))}}{\sigma_R f_R(\widetilde{Q}_\tau)}. \tag{4.6}$$

To see that the HJ bound is always stronger than the local bound, minimize (4.6) with respect to τ. We can show that the minimizer τ^* satisfies $\widetilde{Q}_{\tau^*} = \mu_R$.[14] For

[13] Notice that this is the marginal density under physical measure $\mathbb{P}$.

[14] To see this, write $x = \widetilde{Q}_\tau$, and use $F(\cdot)$ to denote the physical CDF of R. I also drop the R subscript for f to avoid notational clutter. Consider

$$\Gamma(x) = \frac{F(x)(1-F(x))}{f(x)^2}.$$

Minimizing $\Gamma(x)$ is equivalent to minimizing (4.6) and first order conditions imply that the optimal x^* satisfies

$$[f(x^*) - 2F(x^*)f(x^*)]f(x^*)^2 - 2f(x^*)f'(x^*)[F(x^*)(1-F(x^*))] = 0. \tag{4.7}$$

this choice, $\phi(\tau^*) = \mathbb{P}(R \leq \widetilde{Q}_{\tau^*}) = 1/2$ and $f_R(\widetilde{Q}_{\tau^*}) = 1/\sqrt{2\pi\sigma_R^2}$. Therefore, (4.6) obeys the bound

$$\frac{\sqrt{\phi(\tau)(1-\phi(\tau))}}{\sigma_R f(\widetilde{Q}_\tau)} \geq \frac{\sqrt{2\pi}}{2} \approx 1.25.$$

Hence, the HJ bound is always stronger in a model where the SDF and return are jointly normal.

Example 4.3 (Joint lognormality)**.** Let Z_R and Z_M be standard normal random variables with correlation ρ and consider the specification

$$R = e^{(\mu_R - \frac{\sigma_R^2}{2})\lambda + \sigma_R\sqrt{\lambda}Z_R}$$
$$M = e^{-(r_f + \frac{\sigma_M^2}{2})\lambda + \sigma_M\sqrt{\lambda}Z_M},$$

where λ governs the time scale. Simple algebra shows that the no-arbitrage condition, $\mathbb{E}[RM] = 1$, is satisfied when $\mu_R - r_f = -\rho\sigma_R\sigma_M$. It is hard to find an analytical solution for the relative efficiency between the HJ and local bound in this case, but linearization leads to a closed form expression which is quite accurate in simulations. The details are described in Appendix A.4, where I prove that

$$\min_{\tau\in(0,1)} \frac{\text{HJ bound}}{\text{Local bound}} \approx \frac{1}{2}\sqrt{\frac{2\pi\sigma_R^2\lambda}{\exp(\sigma_R^2\lambda) - 1}}. \tag{4.8}$$

This expression is independent of μ_R. An application of l'Hôspital's rule reveals that the relative efficiency converges to $\sqrt{2\pi}/2$ if $\lambda \to 0^+$.[15] The ratio in (4.8) is less than 1 if $\sigma \geq 0.92$ and $\lambda = 1$. If $R = R_m$ (the market return), and the annualized market return volatility is about 16%, then the HJ bound is stronger than the local bound under any reasonable parameterization if the SDF and market return are lognormal.

Example 4.4 (Pareto distribution)**.** I now give an example of a model where the local bound can be stronger than the HJ bound, due to the fat tails of the return distribution. Let $U \sim \textbf{Unif}[0,1]$ (Uniform distribution on [0,1]) and consider the following specification:

$$M = AU^\alpha, \; R = BU^{-\beta} \qquad \text{with} \qquad \alpha, \beta, A, B > 0. \tag{4.9}$$

A random variable $X \sim \textbf{Par}(C, \zeta)$ follows a Pareto distribution with scale parameter

Since f, F are the respective PDF and CDF of the normal random variable R, it follows that $f'(\mu_R) = 0$ and $F(\mu_R) = 1/2$. As a result, (4.7) holds when $\widetilde{Q}_{\tau^*} = x^* = \mu_R$.

[15] This is the same relative efficiency in Example 4.2, which is unsurprising as the linearization becomes exact in the limit as $\lambda \to 0^+$.

$C > 0$ and shape parameter $\zeta > 0$ if the CDF is given by

$$\mathbb{P}(X \leq x) = \begin{cases} 1 - (x/C)^{-\zeta} & x \geq C \\ 0 & x < C. \end{cases}$$

The assumption (4.9) implies that returns follow a Pareto distribution, both under the physical and risk-neutral measure. This fact allows me to obtain an explicit expression for the local bound. I summarize these properties in the Proposition below.

Proposition 4.2. *Let the SDF and return be given by (4.9). Then,*

(i) Under $\mathbb{P}$, the distribution of returns is Pareto: $R \sim \mathbf{Par}(B, 1/\beta)$.

(ii) Under $\widetilde{\mathbb{P}}$, the distribution of returns is Pareto: $R \sim \mathbf{Par}\left(B, \frac{\alpha+1}{\beta}\right)$.

(iii) The Sharpe ratio on the asset return is given by

$$\frac{\mathbb{E}[R] - R_f}{\sigma(R)} = \frac{\frac{B}{1-\beta} - \frac{\alpha+1}{A}}{\sqrt{\frac{B^2}{1-2\beta} - \left(\frac{B}{1-\beta}\right)^2}}. \tag{4.10}$$

(iv) The local bound is given by

$$\frac{1}{R_f} \frac{|\tau - \phi(\tau)|}{\sqrt{\phi(\tau)(1-\phi(\tau))}} = \frac{A}{1+\alpha} \frac{\left|\tau - 1 + (1-\tau)^{\frac{1}{\alpha+1}}\right|}{\sqrt{(1-(1-\tau)^{\frac{1}{\alpha+1}})(1-\tau)^{\frac{1}{\alpha+1}}}}.$$

(v) If $\beta \uparrow \frac{1}{2}$, then the HJ bound converges to 0.

Proof. See Appendix A.5. ■

Proposition 4.2 shows that the local bound is independent of the Pareto tail index β. Properties (iv) and (v) provide some intuition when the local bound is stronger than the HJ bound. Namely, heavier tails of the distribution of R (as measured by β) lead to a lower Sharpe ratio. However, the local bound is unaffected by β since it only depends on the tail index α. Therefore, when β gets close to 1/2, the HJ bound is rather uninformative whereas the local bound may fare better. Moreover, we do not need to impose any restrictions on the parameter space to calculate the local bound, while the HJ bound requires $\beta < 1/2$.[16]

Figure 2 shows two instances of the local and HJ bound using different parameter calibrations. Both calibrations are targeted to match an equity premium of 8% and

[16]The latter restriction is not unreasonable for asset returns, since typical tail index estimates suggest $\beta \in [1/4, 1/3]$ (Danielsson and de Vries, 2000).

risk-free rate of 0%. However, in Panel (b), the distribution of returns has a fatter tail compared to Panel (a). In both calibrations, the local bound has a range of values for which it is stronger than the HJ bound. In line with Proposition 4.2, we see that the range is larger in Panel (b), since the HJ bound is less informative owing to the heavier tails of R.

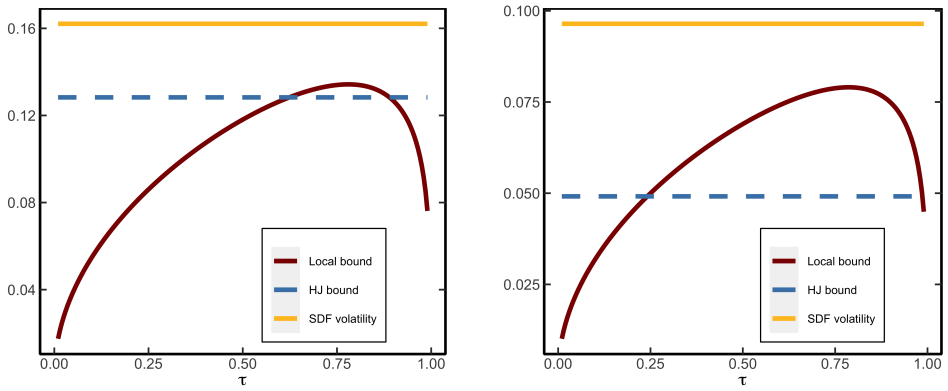

(a) $\beta = 0.33$ (b) $\beta = 0.45$

Figure 2: **Local and HJ bound for heavy tailed returns**. Both panels plot the local bound, HJ bound and true SDF volatility for the Pareto model (4.9). In Panel (b), the distribution of returns has a fatter tail compared to Panel (a). Panel (a) uses the parameters $[A, \alpha, B, \beta] = [1.19, 0.19, 0.72, 0.33]$. Panel (b) uses the parameters $[A, \alpha, B, \beta] = [1.11, 0.11, 0.59, 0.45]$. Both calibrations imply an equity premium of 8% and (net) risk-free rate of 0%.

Example 4.5 (Disaster risk)**.** The disaster risk model of Rietz (1988) and Barro (2006) posits that risk premia are driven by extreme events that affect consumption growth. I follow the specification (and calibration) in Backus et al. (2011), who assume that the representative agent has power utility and the log pricing kernel is given by

$$\log M = \log(\beta) - \gamma \Delta c.$$

Innovations in consumption growth are driven by two independent shocks

$$\Delta c = \varepsilon + \eta, \tag{4.11}$$

where $\varepsilon \sim N(\mu, \sigma^2)$ and

$$\eta | (J = j) \sim N(j\theta, j\nu^2), \quad J \sim \textbf{Poisson}(\kappa).$$

The interpretation of η is that of a jump component (disaster) which induces negative shocks to consumption growth and κ governs the jump intensity for the Poisson distribution. The market return is considered as a claim on levered consumption, i.e. an asset that pays dividends C^λ. I convert the model implied volatility bounds

to monthly units, to facilitate the comparison with the long-run risk model and the empirical bounds obtained in Section 5.2. The local bound, HJ bound and SDF volatility are illustrated in Figure 3a.[17] We see that the local bound has a sharp peak at $\tau = 0.046$, after which it decreases monotonically. Interestingly, there is a range of τ values for which the local bound is sharper than the HJ bound.

This result can be understood from the physical and risk-neutral distribution in Figure 1a.[18] The risk-neutral distribution displays a heavy left tail, owing to the implied disaster risk embedded in the SDF. As a result, it is extremely profitable to sell digital put options which pay out in case of a disaster. These put options must have high Sharpe ratios as their prices are high (insurance against disaster risk), but the actual probability of disaster is low enough that the risk associated to selling such insurance is limited.

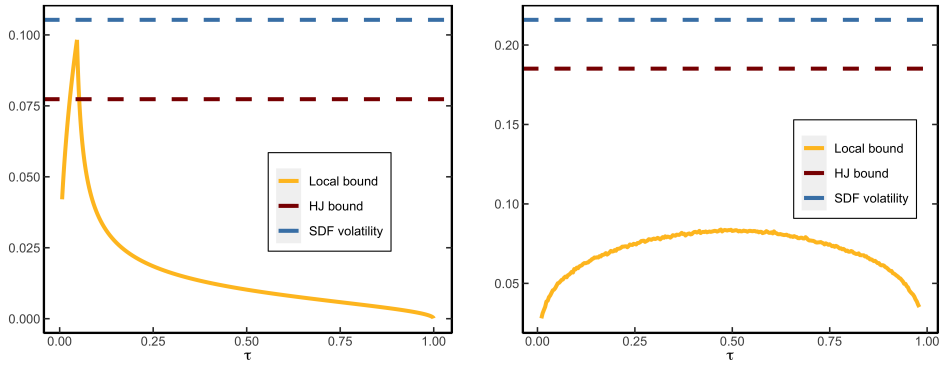

(a) Disaster risk (b) Long-run risk

Figure 3: **HJ and local bound for disaster risk and long-run risk model.** Panels (a) and (b) show the HJ and local bound for the disaster risk and long-run risk model respectively. The bounds and true SDF volatility are in monthly units.

Example 4.6 (Long-run risk)**.** The long-run risk (LRR) model of Bansal and Yaron (2004) posits that consumption growth is driven by a small and persistent component that captures long-run risk. After calibration, this model is successful in matching many of the salient features of the US market return. I consider the extended model (and calibration) of Bansal et al. (2012), which allows for correlation between consumption growth shocks and dividend growth. The local bound, as well as the HJ bound and SDF volatility are estimated by simulation, using 110,000 months, where the first 10,000 observations are dropped as burn-in sample. The results are summarized in Figure 3b. Unlike the disaster risk model, the local bound is always weaker

[17] The bounds can be calculated analytically, see Appendix A.6 for the details.

[18] The right tail of the distributions is not shown, since the distributions are virtually indistinguishable in that region.

than the HJ bound. Moreover, owing to the lognormal assumption, the local bound is almost symmetric around $\tau = 0.5$, at which the maximum is attained.

5 Local Bound in the Data

In this section, I estimate the local bound on monthly return data and discuss it's use in detecting model misspecification.

5.1 Estimation of the Local Bound

I estimate the local bound (4.2) on 30-day S&P500 returns, which are *non-overlapping* and span the period 1996–2021. The returns are sampled at the middle of each month and constitute a total of 312 observations. The Sharpe ratio over this period is 13%, hence the HJ bound tells us that the (monthly) SDF is quite volatile. The local bound consists of three unknowns that need to be estimated: the physical distribution F, the risk-neutral quantile function $\widetilde{Q}_\tau$, and the risk-free rate R_f. I estimate the unconditional risk-free rate, denoted by $\bar{R}_f$, based on the average historical monthly interest rates.

Let $N = 30$, so that $R_{m,t\to N}$ denotes the monthly return on the S&P500 index. Since $R_{m,t\to N}$ is drawn from the physical distribution, we can estimate F based on historical returns using a kernel CDF estimator

$$\widehat{F}(x) \coloneqq \frac{1}{T}\sum_{t=1}^{T} \Phi\left(\frac{x - R_{m,t\to N}}{h}\right), \tag{5.1}$$

where $\Phi(\cdot)$ is the Epanechnikov kernel and h is the bandwidth. I use a kernel CDF estimator to ensure that the local bound is a smooth function of τ. Imposing a smooth local bound improves the approximation in finite samples and mitigates the influence of outliers that would be more pronounced if, say, we use the discontinuous empirical CDF estimator. The optimal bandwidth is determined via cross-validation.

Second, I use the same procedure from Section 3.2 to estimate the conditional risk-neutral CDF $\widetilde{F}_t$. Subsequently, I average the conditional distributions to estimate the unconditional CDF:

$$\widehat{\widetilde{F}}(x) \coloneqq \frac{1}{T}\sum_{t=1}^{T} \widetilde{F}_t(x).$$

Under suitable restrictions on the distribution of returns, we expect $\widehat{\widetilde{F}}$ to converge to $\widetilde{F}$ as $T \to \infty$. An estimate of the unconditional risk-neutral quantile curve is then

obtained from

$$\widehat{\widetilde{Q}}(\tau) \coloneqq \inf\left\{x \in \mathbb{R} : \tau \leq \widehat{\widetilde{F}}(x)\right\}. \tag{5.2}$$

Based on the physical CDF (5.1) and risk-neutral quantile function (5.2), I estimate the local bound by

$$\widehat{\theta}(\tau) \coloneqq \frac{\left|\tau - \widehat{\phi}(\tau)\right|}{\sqrt{\widehat{\phi}(\tau)(1-\widehat{\phi}(\tau))}\widehat{R}_f}, \qquad \tau \in [\varepsilon, 1-\varepsilon] \subseteq (0,1), \tag{5.3}$$

where $\widehat{\phi}(\tau) \coloneqq \widehat{F}(\widehat{\widetilde{Q}}(\tau))$ is the estimated ODC and ε is a small positive number.

5.2 Local Bound for S&P500 Returns

Figure 4a shows the physical and risk-neutral CDF in the data. In line with the disaster risk model in Figure 1a, we see that the physical and risk-neutral CDF differ most in the left tail. The local bound shows that this difference leads to a volatile SDF, which is shown in Figure 4b. The lower bound on the SDF volatility implied by the local bound is much stronger than the HJ bound in the left tail. This finding is consistent with empirical evidence which documents that high Sharpe ratios can be attained by selling out-of-the money put options (see Broadie et al. (2009) and the references therein). The local bound shows that high SDF volatility comes from the local difference between the physical and risk-neutral distribution around the 5^{th} percentile. The non-monotonicity in the right tail of the local bound occurs because $\widetilde{F}(x) > F(x)$, for x large enough. That is, the physical distribution does not first-order stochastically dominates the risk-neutral distribution.[19]

The graphical evidence suggests that the local bound renders a stronger bound on the SDF volatility than the HJ bound. To test this hypothesis more formally, I fix a priori the probability level at 0.046 ($\tau = 0.046$), which renders the sharpest bound on the SDF volatility in the disaster risk model (Example 4.5). At this probability level, the local bound is 30% in the data, which is more than twice as high as the HJ bound. To see whether this difference is statistically significant, I consider the following test statistic

$$\mathcal{T} \coloneqq \widehat{\theta}(0.046) - \frac{\left|\bar{R}_m - \bar{R}_f\right|}{\widehat{\sigma}\bar{R}_f}. \tag{5.4}$$

The first term on the right denotes the estimated local bound (5.3) evaluated at the 4.6^{th} percentile, using the entire time series of returns $\{R_{m,t\to N}\}$. The second term denotes the estimated HJ bound, using $\bar{R}_m$ and $\widehat{\sigma}$ as the respective sample mean

[19] This result is consistent with Table 1, where I formally reject the null hypothesis that the physical distribution first-order stochastically dominates the risk-neutral distribution.

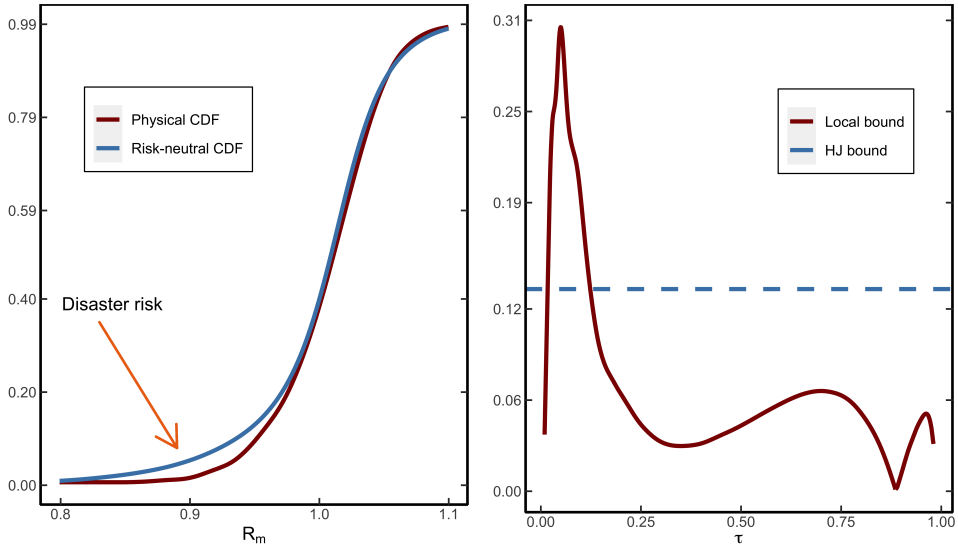

(a) (b)

Figure 4: **Physical/risk-neutral CDF and local bound for monthly S&P500 returns**. Panel (a) shows the unconditional phyisical and risk-neutral CDF for monthly S&P500 returns, over the period 1996-2021. Panel (b) shows the local bound as function of τ, together with the HJ bound.

and standard deviation of $\{R_{m,t\to N}\}$. A value of $\mathcal{T} > 0$ indicates that the local bound is stronger than the HJ bound. To test this restriction, consider the null and alternative hypothesis:

$$\begin{aligned} H_0 &: \mathcal{T} \leq 0 \\ H_1 &: \mathcal{T} > 0. \end{aligned} \tag{5.5}$$

Since the distribution of (5.4) is hard to characterize, I use stationary bootstrap to approximate the p-value under the null hypothesis. The stationary bootstrap is used to generate time indices from which we recreate (with replacement) bootstrapped returns $\{R^{\star}_{m,t\to N}\}$ (Politis and Romano, 1994). The same bootstrapped time indices are used to re-estimate the physical CDF and risk-neutral quantile function. I repeat the bootstrap exercise 100,000 times and for each bootstrap sample, I calculate the test statistic $\mathcal{T}^{\star}$. Finally, the empirical p-value is obtained as the fraction of times $\mathcal{T}^{\star} \leq 0$. The last column in Table 3 shows that the p-value is 6%, which is at the borderline of rejecting H_0.

When the HJ bound is stronger than the local bound, many of the bootstrap samples may not have disaster shocks. Specifically, when considering bootstrap samples with at least one month where returns are less than -20%, the p-value is only

4%. It is important to note that in the sample, there are only two instances where returns are less than -20%: in September 2008 and February 2020. However, the p-value increases to 20% for bootstrap samples that do not include these months. These findings highlight the sensitivity of the test to the presence of disaster shocks.

Table 3: **Sample bounds and bootstrap result**

Sample size	HJ bound	local bound	p-value
312	0.13	0.30	0.06

Note: This table reports the HJ and local bound for monthly S&P500 returns over the period 1996–2021. The local bound is evaluated at $\tau = 0.0464$. The final column denotes the p-value of the null hypothesis in (5.5). The p-value is obtained from 100,000 bootstrap samples and counts the fraction of times that $\mathcal{T}^\star \leq 0$.

5.3 Model implications

As demonstrated in the previous section, the local bound is sharper than the HJ bound, which poses a new challenge for asset pricing models. For instance, in Section 4.2, it was argued that any model that assumes joint normality between the SDF and return cannot generate a stronger local bound. This conclusion also applies to lognormal models under reasonable calibration, as long as the time horizon is not too long. The reason is that the tails of the physical and risk-neutral distributions are nearly indistinguishable. However, empirical evidence in Figure 4 shows substantial disparity between both distributions in the left tail. The LRR model of Bansal et al. (2012) cannot account for a higher local bound under typical calibration, given that the SDF and market return are lognormal. Fixing all parameters of the model, simulation suggests that a risk aversion coefficient of 90 is necessary for the local bound to exceed the HJ bound, a level that is unreasonably high.

The shape of the local bound can also serve as a useful tool for analyzing misspecification. In particular, the empirical local bound is markedly asymmetric, with a notably weaker right tail than the HJ bound. The disaster risk model predicts exactly the same behavior, as it assumes that shocks to the market are negative conditional on a jump. This assumption implies that the physical and risk-neutral distributions differ mainly in the left tail, resulting in an asymmetry in the local bound. In contrast, the lognormal assumption implies that the local bound is almost symmetrical, with the physical and risk-neutral distributions differing primarily around the median. These empirical findings highlight the importance of incorporating disaster risk in asset pricing models, and a local analysis based on the local bound is essential for revealing this stylized fact.

6 Lower bound on physical quantile and dark matter

The results in Section 3 and 5.2 show that the risk-neutral quantile is not a good approximation to the physical quantile function in the left tail. I now derive a risk-adjustment term that better approximates $Q_{t,\tau}$. The latent quantile function $Q_{t,\tau}$ in the left tail is of direct interest, since it gives a measure of *conditional disaster risk*.

To analyze the difference between $Q_{t,\tau}$ and $\widetilde{Q}_{t,\tau}$, I use some elementary tools from functional analysis. The quantile function can be regarded as a map φ between normed spaces, taking as input a distribution function and returning the quantile function: $\varphi(F_t) = F_t^{-1} = Q_{t,\tau}$. Expanding φ around the observed risk-neutral CDF yields

$$Q_{t,\tau} - \widetilde{Q}_{t,\tau} = \varphi(F_t) - \varphi(\widetilde{F}_t) = \varphi'_{\widetilde{F}_t}(F_t - \widetilde{F}_t) + o\left(\left\|F_t - \widetilde{F}_t\right\|\right), \tag{6.1}$$

where $\|\cdot\|$ is a norm on a suitable linear space[20] and $\varphi'_{\widetilde{F}_t}(F_t - \widetilde{F}_t)$ is the Gâteaux derivative of φ at $\widetilde{F}_t$ in the direction of F_t:

$$\begin{aligned}\varphi'_{\widetilde{F}_t}(F_t - \widetilde{F}_t) &:= \lim_{\lambda \downarrow 0} \frac{\varphi\left[(1-\lambda)\widetilde{F}_t + \lambda F_t\right]}{\lambda} \\ &= \frac{\partial}{\partial \lambda} \varphi\left((1-\lambda)\widetilde{F}_t + \lambda F\right)\Big|_{\lambda=0}.\end{aligned} \tag{6.2}$$

Heuristically, the Gâteaux derivative can be thought of as measuring the change in the quantile function when we move the risk-neutral distribution in the direction of the physical distribution. Appendix A.7 shows that the Gâteaux derivative is given by

$$\varphi'_{\widetilde{F}_t}(F_t - \widetilde{F}_t) = \frac{\tau - F_t(\widetilde{Q}_{t,\tau})}{\widetilde{f}_t(\widetilde{Q}_{t,\tau})} = \frac{\tau - \phi_t(\tau)}{\widetilde{f}_t(\widetilde{Q}_{t,\tau})}, \tag{6.3}$$

where $\phi_t(\tau) = F_t(\widetilde{Q}_{t,\tau})$ denotes the conditional ODC. I proceed under the working hypothesis that the remainder term in (6.1) is "small" in the sup-norm, $\|g\|_\infty = \sup_x |g(x)|$.

Assumption 6.1. *The remainder term in (6.1) can be neglected.*

Remark. I simply assume that the first order approximation in (6.1) is accurate. The assumption that $||F_t - \widetilde{F}_t||_\infty$ is small can be understood as excluding near-arbitrage opportunities, since the local bound in Theorem 4.1 shows that substantial pointwise difference between $F_t(\cdot)$ and $\widetilde{F}_t(\cdot)$ leads to a very volatile SDF. Appendix

[20] Formally, the space can be defined as $\{\Delta : \Delta = c(F-G), F, G \in \mathbb{D}, c \in \mathbb{R}\}$ and $\mathbb{D}$ is the space of distribution functions (Serfling, 2009). See van der Vaart (2000, Section 20.1) and Serfling (2009, p. 217) for further details about the approximation.

E.3 illustrates the approximation in the Black and Scholes (1973) model.

I combine (6.1) and (6.3) in conjunction with Assumption 6.1 to obtain the approximation

$$Q_{t,\tau} \approx \widetilde{Q}_{t,\tau} + \underbrace{\frac{\tau - F_t(\widetilde{Q}_{t,\tau})}{\widetilde{f}_t(\widetilde{Q}_{t,\tau})}}_{\text{risk-adjustment}}. \tag{6.4}$$

The approximation in (6.4) contains the terms $\widetilde{Q}_{t,\tau}$ and $\widetilde{f}_t(\widetilde{Q}_{t,\tau})$, which are directly observed at time t using (a variation of) the Breeden and Litzenberger (1978) formula in (3.2). However, the physical CDF is unknown and hence (6.4) cannot be used directly to approximate $Q_{t,\tau}$.

To make further progress, I show that the numerator term, $\tau - F_t(\widetilde{Q}_{t,\tau})$, can be bounded with option data under certain economic constraints. Chabi-Yo and Loudis (2020) show that in representative agent models, the SDF is a function of the market return:

$$\frac{\mathbb{E}_t\left[M_{t\to N}\right]}{M_{t\to N}} = \frac{\frac{u'(W_t x_0)}{u'(W_t x)}}{\widetilde{\mathbb{E}}_t\left[\frac{u'(W_t x_0)}{u'(W_t x)}\right]} \qquad \text{with } x = R_{m,t\to N} \text{ and } x_0 = R_{f,t\to N}, \tag{6.5}$$

where W_t is the agent's wealth at time t and $u(x)$ is the utility function. Define

$$\zeta(x) \coloneqq \frac{u'(W_t R_{f,t\to N})}{u'(W_t x)} \quad \text{and} \quad \theta_k = \frac{1}{k!}\left(\frac{\partial^k \zeta(x)}{\partial x^k}\right)_{x=R_{f,t\to N}}. \tag{6.6}$$

I make the following assumptions about the market return and the utility function of the representative agent.

Assumption 6.2. *(i)* $\widetilde{\mathbb{E}}_t\left[R^4_{m,t\to N}\right] < \infty$. *(ii)* $\zeta^{(4)}(x) \leq 0$. *(iii) The following integrability condition holds*

$$\int_0^1 \zeta^{(4)}(R_{f,t\to N}(1-s))\,(1-s)^3\,\mathrm{d}s < \widetilde{\mathbb{E}}_t\left[G(R_{m,t\to N})\right] \quad \text{or} \quad \zeta^{(4)}(x) = 0, \tag{6.7}$$

where

$$G(x) = \frac{(x - R_{f,t\to N})^4}{4!}\int_0^1 \zeta^{(4)}(R_{f,t\to N} + s(x - R_{f,t\to N}))\,(1-s)^3\,\mathrm{d}s.$$

Part (i) allows for fat tails in the risk-neutral distribution as long as the kurtosis is finite. Chabi-Yo and Loudis (2020) present sufficient conditions for part (ii) to hold, which relate to the sign of the nth derivative of the utility function of the representative agent. Part (iii) is sufficient to establish the lower bound in Theorem 6.3 below. I show that (iii) holds for some common utility functions in Section A.8.1.

The second condition in (6.7) is needed to deal with special cases such as log utility.

Under Assumption 6.2, we can bound the difference between the physical and risk-neutral distribution.

Theorem 6.3 (Infeasible lower bound)**.** *Let Assumption 6.2 hold and assume that the risk-neutral CDF is absolutely continuous with respect to Lebesgue measure. Define τ^* so that $G(\widetilde{Q}_{t,\tau^*}) = G(R_{m,t\to N})$. Then for all $\tau \leq \tau^*$,*

$$\tau - F_t\left(\widetilde{Q}_{t,\tau}\right) \geq \frac{\sum_{k=1}^3 \theta_k \left(\tau \widetilde{\mathbb{M}}_{t\to N}^{(k)} - \widetilde{\mathbb{M}}_{t\to N}^{(k)}[\widetilde{Q}_{t,\tau}]\right)}{1 + \sum_{k=1}^3 \theta_k \widetilde{\mathbb{M}}_{t\to N}^{(k)}}, \tag{6.8}$$

where

$$\begin{aligned} \widetilde{\mathbb{M}}_{t\to N}^{(n)} &:= \widetilde{\mathbb{E}}_t\left[(R_{m,t\to N} - R_{f,t\to N})^n\right] \\ \widetilde{\mathbb{M}}_{t\to N}^{(n)}[k_0] &:= \widetilde{\mathbb{E}}_t\left[\mathbb{1}\left(R_{m,t\to N} \leq k_0\right)(R_{m,t\to N} - R_{f,t\to N})^n\right]. \end{aligned} \tag{6.9}$$

Proof. See Appendix A.8. ∎

The (un)truncated moments in (6.9) can be computed from option prices (see Appendix A.9), but the bound in (6.8) is still infeasible since θ_k is unknown.[21] However, Chabi-Yo and Loudis (2020, Table 6) provide empirical evidence that

$$\theta_1 = \frac{1}{R_{f,t\to N}}, \theta_2 = -\frac{1}{R_{f,t\to N}^2}, \text{ and } \theta_3 = \frac{1}{R_{f,t\to N}^3}. \tag{6.10}$$

Under (6.10), I can obtain a feasible bound on $\tau - F_t\left(\widetilde{Q}_{t,\tau}\right)$.

Corollary 6.4 (Feasible lower bound)**.** *Suppose the assumptions of Theorem 6.3 hold. In addition, suppose that (6.10) holds. Then for all $\tau \leq \tau^*$,*

$$\tau - F_t\left(\widetilde{Q}_{t,\tau}\right) \geq \frac{\sum_{k=1}^3 \frac{(-1)^{k+1}}{R_{f,t\to N}^k} \left(\tau \widetilde{\mathbb{M}}_{t\to N}^{(k)} - \widetilde{\mathbb{M}}_{t\to N}^{(k)}[\widetilde{Q}_{t,\tau}]\right)}{1 + \sum_{k=1}^3 \frac{(-1)^{k+1}}{R_{f,t\to N}^k} \widetilde{\mathbb{M}}_{t\to N}^{(k)}} =: \mathrm{LB}_{t,\tau}. \tag{6.11}$$

Proof. See Appendix A.8. ∎

Corollary 6.5. *Under the same assumptions of Corollary 6.4 and assuming that the remainder term in (6.4) is negligible, we have*

$$Q_{t,\tau} - \widetilde{Q}_{t,\tau} \geq \overbrace{\frac{\mathrm{LB}_{t,\tau}}{\widetilde{f}_t(\widetilde{Q}_{t,\tau})}}^{\text{risk-adjustment}} =: \mathrm{RA}_{t,\tau}. \tag{6.12}$$

[21] In Appendix C, I provide closed form expressions of (A.21) for commonly used utility functions. These expressions generalize the equity premium results of Martin (2017) and Chabi-Yo and Loudis (2020) to the whole distribution.

The bound in Corollary 6.4 does not require any parameter estimation and can be calculated solely based on time t information. Corollary 6.4 complements the recent literature on the recovery of beliefs. Ross (2015) shows that one can recover F_t, if the pricing kernel is transition independent. Subsequent work (Borovička et al., 2016; Qin et al., 2018; Jackwerth and Menner, 2020) casts doubt on the transition independence assumption and shows that recovery is generally impossible. Complimentary to these results, Corollary 6.4 shows that one can still establish a lower bound on the left tail of the physical distribution, using a different set of (mild) economic constraints. Moreover, Section 3.3 showed that the right tail of F_t can be recovered from the risk-neutral distribution due to the near absence of risk-adjustment. Both results combined show that approximate recovery of F_t using option prices might still possible.

Corollary 6.5 establishes a lower bound on the difference between the physical and risk-neutral quantile function, which can be thought of as a risk-adjustment term. If the lower bound in (6.12) happens to be tight, it gives us a direct measure of conditional disaster risk. In addition, the term on the right of (6.12) is not subject to the historical sample bias critique of Welch and Goyal (2008) and it is available at a daily frequency. The motivation for introducing disaster risk is to explain the historically high equity premium (Rietz, 1988; Barro, 2006). However, a high (conditional) equity premium does not necessarily arise due to disaster risk and, moreover, calibrating these models is difficult due to the lack of disasters in the data (Martin, 2013). For these reasons, it is of interest to approximate $Q_{t,\tau}$ in the left tail using a model-free approach. The next Section shows that the assumption of a tight lower bound in (6.12) cannot be rejected, which allows me to obtain a model-free measure of disaster risk.

6.1 How tight is the lower bound in Corollary 6.5?

6.1.1 Estimation of the lower bound

I first outline the procedure to calculate $\text{LB}_{t,\tau}$ and $\widetilde{f}_t(\widetilde{Q}_{t,\tau})$, which are needed to compute the lower bound in Corollary 6.5. Since $\frac{d}{d\tau}\widetilde{Q}_t(\tau) = 1/\widetilde{f}_t(\widetilde{Q}_{t,\tau})$, I approximate the denominator term in (6.12) by

$$\frac{1}{\widetilde{f}_t(\widetilde{Q}_{t,\tau})} \approx \frac{\widetilde{Q}_t(\tau+h) - \widetilde{Q}_t(\tau-h)}{2h},$$

where h is the bandwidth of the τ-grid.[22] Second, to calculate $\text{LB}_{t,\tau}$ from (6.11), I use the estimated quantile curve $\widetilde{Q}_{t,\tau}$ in combination with the formula for high order risk-neutral moments in Appendix A.9.

Since virtually all macro-finance models assume that the market return is negatively correlated with the SDF, one expects the market return to have a higher probability of a crash under risk-neutral measure than under physical measure. This means that Corollary 6.5 has non trivial content if $\text{LB}_{t,\tau} \geq 0$ in the data. I confirm that $\text{LB}_{t,\tau} \geq 0$ for all dates considered, using the same τ's from Table 5 below. Appendix Table E1 contains summary statistics of $\text{RA}_{t,\tau}$, which show that the risk-adjustment term is right-skewed, more pronounced in the right tail and economically meaningful in magnitude, with outliers that can spike up to 29%.

6.1.2 In-sample predictive performance

To test whether the lower bound in Corollary 6.5 is tight, I form *excess quantile returns*: $R_{m,t\to N} - \widetilde{Q}_{t,\tau}$. Since $\widetilde{Q}_{t,\tau}$ is observed at time t, we have $Q_{t,\tau}(R_{m,t\to N} - \widetilde{Q}_{t,\tau}) = Q_{t,\tau}(R_{m,t\to N}) - \widetilde{Q}_{t,\tau}$. Subsequently, I use QR to estimate the model

$$Q_{t,\tau}(R_{m,t\to N}) - \widetilde{Q}_{t,\tau}(R_{m,t\to N}) = \beta_0(\tau) + \beta_1(\tau)\text{RA}_{t,\tau}, \tag{6.13}$$

$$[\widehat{\beta}_0(\tau), \widehat{\beta}_1(\tau)] = \underset{\beta_0,\beta_1\in\mathbb{R}}{\arg\min} \sum_{t=1}^{T} \rho_\tau(R_{m,t\to N} - \widetilde{Q}_{t,\tau} - \beta_0 - \beta_1\text{RA}_{t,\tau}).$$

Regression (6.13) is similar to the excess return regressions of Welch and Goyal (2008). Under the null hypothesis that the lower bound is tight, we have

$$H_0: \qquad [\beta_0(\tau), \beta_1(\tau)] = [0, 1]. \tag{6.14}$$

Less restrictive, we can test whether $\beta_0(\tau) = 0$ and $\beta_1(\tau) > 0$, which implies that the statistical "factor" $\text{RA}_{t,\tau}$ explains the conditional quantile wedge.[23]

Table 4 shows the result of regression (6.13). The null hypothesis of a tight lower bound cannot be rejected for $\tau = 0.2$, but is rejected for $\tau \in \{0.05, 0.1\}$ at all horizons. In case the null hypothesis is rejected, the $\beta_1(\tau)$-coefficient is larger than 1, which is consistent with the theory that $\text{RA}_{t,\tau}$ represents a lower bound on the difference between the physical and risk-neutral distribution. Table 4 also documents

[22] I slightly abuse notation to emphasize that the derivative is taken w.r.t. τ, so that $\widetilde{Q}_t(\tau + h)$ denotes $\widetilde{Q}_{t,\tau+h}$.

[23] For example, if we start with a quantile factor model $Q_{t,\tau} = \widetilde{Q}_{t,\tau} + \beta(\tau)\text{RA}_{t,\tau}$, the model has one testable implication for the data: the intercept in a quantile regression of $R_{m,t\to N} - \widetilde{Q}_{t,\tau}$ on $\text{RA}_{t,\tau}$ *should be zero*. Quantile factor models have recently been proposed by Chen et al. (2021).

p-values of the joint hypothesis in (6.14), which again is not rejected for $\tau = 0.2$ only. In all cases, the lower bound is economically meaningful since $\beta_1(\tau)$ is significantly different from 0, while $\beta_0(\tau) = 0$ can never be rejected. To shed more light on the explanatory power of the lower bound, I use the $R^1(\tau)$ measure-of-fit (see (3.5))

$$R^1(\tau) = 1 - \frac{\min_{b_0,b_1} \sum \rho_\tau(R_{m,t\to N} - b_0 - b_1 \mathrm{RA}_{t,\tau})}{\min_{b_0} \sum \rho_\tau(R_{m,t\to N} - b_0)}. \tag{6.15}$$

Table 4 shows that the explanatory power of $\mathrm{RA}_{t,\tau}$ is modest, generally around a few percent. Low explanatory power is typical in the equity premium literature, since high R^2-values lead to high Sharpe ratios, as market timing strategies can be designed to exploit return predictability (Ross, 2005; Campbell and Thompson, 2008). The same logic applies in the quantile case, since the local bound in Theorem 4.1 shows that large pointwise differences between the physical and risk-neutral distribution lead to near arbitrage opportunities. If one could predict this difference, one could again design a trading strategy that exploits the predictability, this time using options rather than a direct timing investment in the market portfolio.

Table 4: **Quantile regression lower bound**

	Horizon (in days)	$\widehat{\beta}_0(\tau)$	$\widehat{\beta}_1(\tau)$	Wald test	$R^1(\tau)$[%]	Obs
$\tau = 0.05$	30	−0.01 (0.006)	4.43 (0.357)	0	6.03	4333
	60	−0.01 (0.018)	5.53 (0.681)	0	3.6	4312
	90	−0.02 (0.040)	6.37 (1.364)	0	4.91	4291
$\tau = 0.1$	30	−0.01 (0.005)	2.17 (0.408)	0.02	3.18	4333
	60	−0.02 (0.016)	3.25 (0.668)	0	2.23	4312
	90	−0.02 (0.024)	3.05 (0.688)	0	4.43	4291
$\tau = 0.2$	30	−0.01 (0.006)	1.33 (0.412)	0.03	0.41	4333
	60	−0.02 (0.012)	1.50 (0.484)	0.47	0.48	4312
	90	−0.02 (0.022)	1.36 (0.704)	0.77	1.46	4291

Note: This table reports the QR estimates of (6.13) over the sample period 2003-2021 at different horizons, using overlapping returns. Standard errors are shown in parentheses and calculated using SETBB with a block length of maturity times 5. *Wald test* denotes the p-value of the joint restriction $[\beta_0(\tau), \beta_1(\tau)] = [0, 1]$. $R^1(\tau)$ denotes the goodness-of-fit measure (6.15).

Another way to test whether the lower bound in Corollary 6.5 represents a mean-

ingful risk-adjustment term is to test directly whether the following is a good proxy for the latent conditional quantile function

$$\widehat{Q}_{t,\tau} = \widetilde{Q}_{t,\tau} + \mathrm{RA}_{t,\tau}. \tag{6.16}$$

I use QR to estimate the model

$$Q_{t,\tau}(R_{m,t\to N}) = \beta_0(\tau) + \beta_1(\tau)\widehat{Q}_{t,\tau}. \tag{6.17}$$

If (6.16) is a good predictor of the conditional quantile function, we have under the null hypothesis

$$H_0: \ \beta_0(\tau) = 0, \quad \beta_1(\tau) = 1. \tag{6.18}$$

Table 5 summarizes the estimates of (6.17) for several quantiles. The results uniformly improve upon the risk-neutral estimates in Table 1. First, the point estimates for $[\beta_0(\tau), \beta_1(\tau)]$ are closer to the $[0, 1]$ benchmark. Second, the Wald test on the joint restriction in (6.18) is never rejected and third, the in-sample explanatory power is higher. The same conclusion applies when comparing the predictive results to the expanding quantile regression from Table 2. These results suggest that $\widehat{Q}_{t,\tau}$ can be regarded as a good proxy for the latent conditional quantile function $Q_{t,\tau}$ in the left tail.

Two additional remarks are in order. First, since we estimate $\widehat{Q}_{t,\tau}$ from option prices, there might be a concern for attenuation bias due to measurement error (Angrist et al., 2006). Appendix E.4 provides simulation evidence which shows that attenuation bias is negligible in a setup that mimics the empirical application. Second, there is a possibility of quantile crossing, which means that the predicted quantiles, $\widehat{\beta}_0(\tau) + \widehat{\beta}_1(\tau)\mathrm{RA}_{t,\tau}$, are not monotone with respect to τ. This problem frequently arises in dynamic quantile models (Gouriéroux and Jasiak, 2008). It appears however, not a concern in our case, since crossing occurs only 0.04% of the time for the 30 day horizon. For the other horizons, crossing happens about 0.1% of the time.[24]

6.1.3 Out-of-sample predictive performance

Since the in-sample results for the physical quantile approximation suggest $\beta_0(\tau) = 0$ and $\beta_1(\tau) = 1$, it is natural to test how well this works out-of-sample by means of predicting $Q_{t,\tau}(R_{m,t\to N})$ directly with $\widehat{Q}_{t,\tau}$, which does not require any parameter estimation.

[24] Recall that the explanatory variable in the estimation, $\mathrm{RA}_{t,\tau}$, changes with the quantile level τ. Hence, based on the estimated coefficients $[\widehat{\beta}_0(\tau), \widehat{\beta}_1(\tau)]$, we cannot tell whether the estimated quantile is monotone in τ.

Table 5: **Risk-adjusted quantile regression**

	Horizon (in days)	$\widehat{\beta}_0(\tau)$	$\widehat{\beta}_1(\tau)$	Wald test	$R^1(\tau)[\%]$	$R^1_{oos}(\tau)[\%]$	Obs
$\tau = 0.05$	30	0.29 (0.267)	0.70 (0.283)	0.09	6.28	9.94	4333
	60	0.30 (0.423)	0.71 (0.472)	0.08	3.4	17.81	4312
	90	0.36 (0.588)	0.64 (0.680)	0.08	4.26	21.98	4291
$\tau = 0.1$	30	0.28 (0.300)	0.72 (0.311)	0.32	3.57	4.02	4333
	60	0.38 (0.457)	0.61 (0.486)	0.23	2.35	9.22	4312
	90	0.31 (0.623)	0.70 (0.676)	0.13	4.19	13.22	4291
$\tau = 0.2$	30	0.57 (0.490)	0.43 (0.498)	0.47	0.58	2.53	4333
	60	0.44 (0.618)	0.56 (0.631)	0.37	0.57	4.28	4312
	90	0.23 (0.767)	0.78 (0.780)	0.58	0.7	5.99	4291

Note: This table reports the QR estimates of (6.17) over the sample period 2003-2021. Standard errors are shown in parentheses and calculated using the SETBB, with block length equal to 5 times the maturity and 1,000 Monte Carlo bootstrap samples. *Wald test* gives the p-value of the Wald test on the joint restriction: $\widehat{\beta}_0(\tau) = 0, \widehat{\beta}_1(\tau) = 1$. $R^1(\tau)$ denotes the in-sample goodness-of fit criterion (3.5). $R^1_{oos}(\tau)$ is the out-of-sample goodness-of fit (6.19), using a rolling window size of $10 \times$ maturity.

In order to interpret $\widehat{Q}_{t,\tau}$ as a valid approximation to the latent quantile function, we need to ensure that $\widehat{Q}_{t,\tau}$ is not subject to the quantile crossing problem. I verify that crossing does not occur for any prediction horizon and quantile level. To asses the out-of-sample performance further, I use the following out-of-sample measure (see (3.6))

$$R^1_{oos}(\tau) = 1 - \frac{\sum \rho_\tau(R_{m,t\to N} - \widehat{Q}_{t,\tau})}{\sum \rho_\tau(R_{m,t\to N} - \overline{Q}_{t,\tau})}. \tag{6.19}$$

The out-of-sample $R^1_{oos}(\tau)$ is also displayed in Table 5. The predictor variable $\widehat{Q}_{t,\tau}$ improves upon the historical rolling quantile out-of-sample in all cases. In particular, this outperformance is most pronounced at the 5^{th} percentile, which is expected since option data are known to provide useful information about extreme downfalls in the stock market (Bates, 2008; Bollerslev and Todorov, 2011). In Appendix E.2, I run a battery of robustness tests which show that, out-of-sample, $\text{RA}_{t,\tau}$ better predicts the quantile than other benchmarks such as the risk-neutral quantile or the VIX index. The latter result is particularly encouraging, since the VIX predictor uses in-sample information.

6.2 Time varying disaster risk and dark matter

The in- and out-of-sample results show that $\widehat{Q}_{t,\tau}$ is a good proxy for the latent conditional quantile function. Time fluctuation in $\widehat{Q}_{t,\tau}$ for small τ can therefore be interpreted as time varying disaster risk. The left panels of Figure 5 show the evolution of $\widehat{Q}_{t,\tau}$ over time for the 30 and 60 day horizon, with $\tau = 0.05$. The time fluctuation in both series is evident from the graph and provides empirical support for the thesis that disaster risk is time-varying, as in the models of Gabaix (2012) and Wachter (2013).

Ross (2015) refers to the impact that changes in perceived disaster probabilities can have on asset prices as *dark matter*: "It is unseen and not directly observable but it exerts a force that can change over time and that can profoundly influence markets". We can illuminate this dark matter somewhat by studying the lowest quantile forecasts in Figure 5, which are produced over the 4$^{\text{th}}$ quarter of 2008 and the Covid crisis. During these periods, the quantile forecasts drop below 72%, which suggests that a loss of -28% or more had an expected probability of 5%. To put things in perspective, it happened only once since 1926 that the S&P500 index recorded a monthly loss of -28% or more.[25] Hence, based on historical estimates, a back of the envelope calculation puts the probability of a loss of -28% or more at 1/1139, which is 57 times lower than 5%.

The right panels of Figure 5 give another view on this dark matter, as they show the evolution of risk-adjustment over time. The largest spikes occur once more at the height of the financial crisis and the difference between the physical and risk-neutral measure can be as large as 25% (30 day horizon) or 16% (60 day horizon). This difference suggests that the risk-neutral quantile decreases disproportionally more than the physical quantile during crises.

It is well known that risk-neutral quantiles are smaller than historical quantiles in the left tail of the distribution. However, this fact alone does not tell us about the market's forecast of a decline, since historical probabilities can be different from the market forecast or the risk-neutral distribution differs significantly from the physical distribution, due to a risk premium on disaster insurance. The discussion above shows that both effects are at play, but the right panels of Figure 5 suggest that the insurance effect is more dominant during a crisis, since the physical and risk-neutral quantile are further apart.

[25] I use historical monthly SP500 return from WRDS that are available from January 1926 and renders a total of 1139 observations.

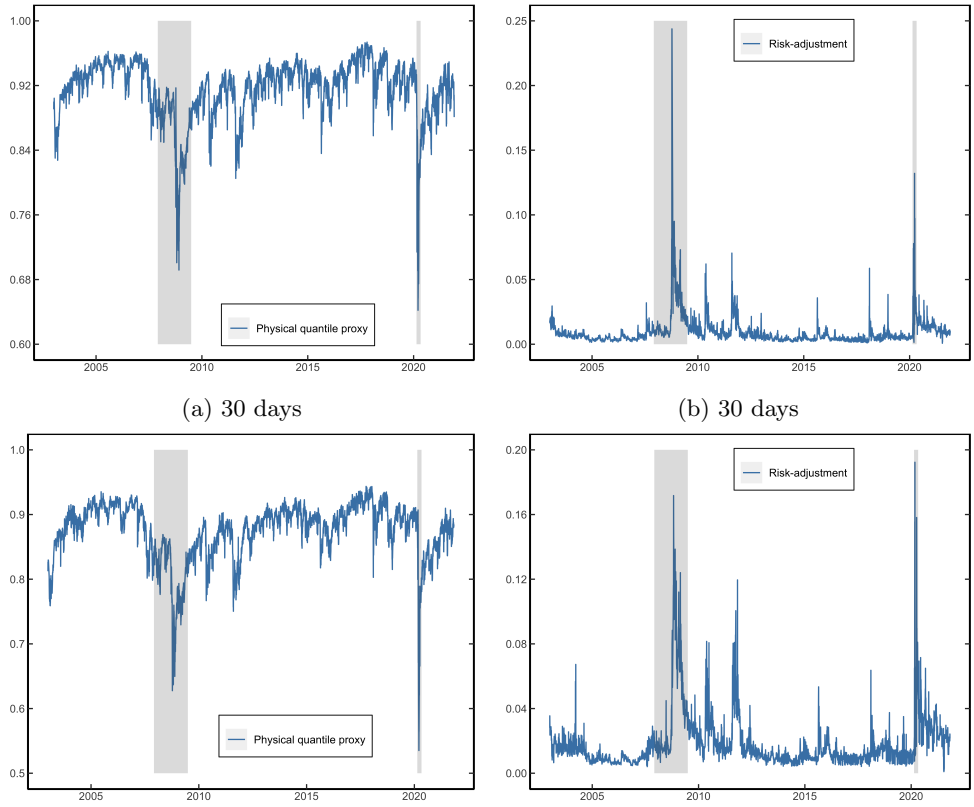

(a) 30 days (b) 30 days

(c) 60 days (d) 60 days

Figure 5: **Time variation in risk-adjustment at the 5^{th} percentile**. The left panels show the real time quantile predictor $\widehat{Q}_{t,\tau}$ from (6.16) for $\tau = 0.05$. The right panels show the risk-adjustment term $\text{RA}_{t,\tau}$ from (6.12). The two shaded bars signify the Great Recession period (Dec 2007 – June 2009) and COVID-19 crisis (Feb 2020 – April 2020).

7 Conclusion

I use return and option data on the S&P500 in combination with quantile regression to obtain a local measure of distance between the physical and risk-neutral distribution. In the data, the difference between both distributions is most pronounced in the left tail, whereas the right tails are nearly indistinguishable.

To build on this finding, I introduce a local bound on the SDF volatility, which demonstrates that the volatility of the SDF is largely driven by local differences in the left tail of the physical and risk-neutral measure. Compared to the closely related HJ bound, the local bound is significantly stronger in the data. An asset pricing model seeking to explain these stylized facts must therefore satisfy two requirements: (i) produce physical and risk-neutral distributions that are similar in the right tail but different in the left tail, and (ii) generate a local bound that is stronger than the HJ

bound in the left tail. These observations pose a challenge to asset pricing models that assume lognormality of the market return and suggest that a disaster (or jump) component is necessary to explain the findings.

Finally, I suggest using a risk-adjustment term observed from option prices to measure the real time difference between the physical and risk-neutral quantile in the left tail. This risk-adjustment term serves as a good predictor of the quantile wedge, exhibiting spikes during crises and significant fluctuations over time, providing preliminary evidence of time-varying disaster risk.

References

Yacine Aït-Sahalia and Andrew W. Lo. Nonparametric estimation of state-price densities implicit in financial asset prices. *Journal of Finance*, 53(2):499–547, 1998. doi:10.1111/0022-1082.215228.

Yacine Aït-Sahalia and Andrew W. Lo. Nonparametric risk management and implied risk aversion. *Journal of Econometrics*, 94(1):9–51, 2000. doi:10.1016/S0304-4076(99)00016-0.

Caio Almeida and René Garcia. Assessing misspecified asset pricing models with empirical likelihood estimators. *Journal of Econometrics*, 170(2):519–537, 2012. doi:10.1016/j.jeconom.2012.05.020.

Fernando Alvarez and Urban J. Jermann. Using asset prices to measure the persistence of the marginal utility of wealth. *Econometrica*, 73(6):1977–2016, 2005. doi:10.1111/j.1468-0262.2005.00643.x.

Joshua Angrist, Victor Chernozhukov, and Iván Fernández-Val. Quantile regression under misspecification, with an application to the U.S. wage structure. *Econometrica*, 74(2):539–563, 2006. doi:10.1111/j.1468-0262.2006.00671.x.

David Backus, Mikhail Chernov, and Ian Martin. Disasters implied by equity index options. *Journal of Finance*, 66(6):1969–2012, 2011. doi:10.1111/j.1540-6261.2011.01697.x.

David Backus, Mikhail Chernov, and Stanley Zin. Sources of entropy in representative agent models. *Journal of Finance*, 69(1):51–99, 2014. doi:10.1111/jofi.12090.

Jushan Bai. Inferential theory for factor models of large dimensions. *Econometrica*, 71(1):135–171, 2003. doi:10.1111/1468-0262.00392.

Gurdip Bakshi, Dilip Madan, and George Panayotov. Returns of claims on the upside and the viability of U-shaped pricing kernels. *Journal of Financial Economics*, 97 (1):130–154, 2010. doi:10.1016/j.jfineco.2010.03.009.

Ravi Bansal and Bruce N. Lehmann. Growth-optimal portfolio restrictions on asset pricing models. *Macroeconomic Dynamics*, 1(2):333–354, 1997. doi:10.1017/S1365100597003039.

Ravi Bansal and Amir Yaron. Risks for the long run: A potential resolution of asset pricing puzzles. *Journal of Finance*, 59(4):1481–1509, 2004. doi:10.1111/j.1540-6261.2004.00670.x.

Ravi Bansal, Dana Kiku, and Amir Yaron. An empirical evaluation of the long-run risks model for asset prices. *Critical Finance Review*, 1(1):183–221, 2012. doi:10.1561/103.00000005.

Andrea Barletta and Paolo Santucci de Magistris. Analyzing the risks embedded in option prices with *rndfittool*. *Risks*, 6(2):1–15, 2018. doi:10.3390/risks6020028.

Robert J. Barro. Rare disasters and asset markets in the twentieth century. *Quarterly Journal of Economics*, 121(3):823–866, 2006. doi:10.1162/qjec.121.3.823.

David S. Bates. The crash of '87: was it expected? The evidence from options markets. *Journal of Finance*, 46(3):1009–1044, 1991. doi:10.1111/j.1540-6261.1991.tb03775.x.

David S. Bates. Post-'87 crash fears in the S&P500 futures option market. *Journal of Econometrics*, 94(1):181–238, 2000. doi:10.1016/S0304-4076(99)00021-4.

David S. Bates. The market for crash risk. *Journal of Economic Dynamics and Control*, 32(7):2291–2321, 2008. doi:10.1016/j.jedc.2007.09.020.

Brendan K. Beare and Lawrence D. W. Schmidt. An empirical test of pricing kernel monotonicity. *Journal of Applied Econometrics*, 31(2):338–356, 2016. doi:10.1002/jae.2422.

Geert Bekaert and Marie Hoerova. The VIX, the variance premium and stock market volatility. *Journal of Econometrics*, 183(2):181–192, 2014. doi:10.1016/j.jeconom.2014.05.008.

Fischer Black and Myron Scholes. The pricing of options and corporate liabilities. *Journal of Political Economy*, 81(3):637–654, 1973. doi:10.1086/260062.

Tim Bollerslev and Viktor Todorov. Tails, fears, and risk premia. *Journal of Finance*, 66(6):2165–2211, 2011. doi:10.1111/j.1540-6261.2011.01695.x.

Jaroslav Borovička, Lars Peter Hansen, and José A Scheinkman. Misspecified recovery. *Journal of Finance*, 71(6):2493–2544, 2016. doi:10.1111/jofi.12404.

Douglas T. Breeden and Robert H. Litzenberger. Prices of state-contingent claims implicit in option prices. *Journal of Business*, 51(4):621–651, 1978. doi:10.1086/296025.

Mark Broadie, Mikhail Chernov, and Michael Johannes. Understanding index option returns. *Review of Financial Studies*, 22(11):4493–4529, 2009. doi:10.1093/rfs/hhp032.

John Y. Campbell and Samuel B. Thompson. Predicting excess stock returns out of sample: Can anything beat the historical average? *Review of Financial Studies*, 21(4):1509–1531, 2008. doi:10.1093/rfs/hhm055.

George Casella and Roger L. Berger. *Statistical Inference*. Duxbury/Thomson Learning. Belmont, CA, 2002.

Fousseni Chabi-Yo and Johnathan Loudis. The conditional expected market return. *Journal of Financial Economics*, 137(3):752–786, 2020. doi:10.1016/j.jfineco.2020.03.009.

Liang Chen, Juan J. Dolado, and Jesús Gonzalo. Quantile factor models. *Econometrica*, 89(2):875–910, 2021. doi:10.3982/ECTA15746.

Victor Chernozhukov, Iván Fernández-Val, and Siyi Luo. Distribution regression with sample selection, with an application to wage decompositions in the UK, 2018. URL `https://arxiv.org/abs/1811.11603`.

John H. Cochrane. *Asset Pricing*. Princeton University Press, 2005.

Joshua D. Coval and Tyler Shumway. Expected option returns. *Journal of Finance*, 56(3):983–1009, 2001. doi:10.1111/0022-1082.00352.

Horatio Cuesdeanu and Jens Carsten Jackwerth. The pricing kernel puzzle in forward looking data. *Review of Derivatives Research*, 21(3):253–276, 2018. doi:10.1007/s11147-017-9140-8.

Jon Danielsson and Casper G. de Vries. Value-at-risk and extreme returns. *Annales d'Économie et de Statistique*, (60):239–270, 2000. doi:10.2307/20076262.

Robert F. Engle and Simone Manganelli. CAViaR: Conditional autoregressive value at risk by regression quantiles. *Journal of Business & Economic Statistics*, 22(4): 367–381, 2004. doi:10.1198/073500104000000370.

Stephen Figlewski. Estimating the implied risk-neutral density for the US market portfolio. In *Volatility and Time Series Econometrics: Essays in Honor of Robert Engle*, chapter 15, pages 323–353. Oxford University Press, 03 2010. doi:10.1093/acprof:oso/9780199549498.003.0015.

Damir Filipović, Eberhard Mayerhofer, and Paul Schneider. Density approximations for multivariate affine jump-diffusion processes. *Journal of Econometrics*, 176(2): 93–111, 2013. doi:10.1016/j.jeconom.2012.12.003.

Xavier Gabaix. Variable rare disasters: An exactly solved framework for ten puzzles in macro-finance. *Quarterly Journal of Economics*, 127(2):645–700, 2012. doi:10.1093/qje/qjs001.

Can Gao and Ian Martin. Volatility, valuation ratios, and bubbles: An empirical measure of market sentiment. *Journal of Finance*, 76(6):3211–3254, 2021. doi:10.1111/jofi.13068.

Christian Gouriéroux and Joann Jasiak. Dynamic quantile models. *Journal of Econometrics*, 147(1):198–205, 2008. doi:10.1016/j.jeconom.2008.09.028.

Karl B. Gregory, Soumendra N. Lahiri, and Daniel J. Nordman. A smooth block bootstrap for quantile regression with time series. *Annals of Statistics*, 46(3): 1138–1166, 2018. doi:10.1214/17-AOS1580.

Lars Peter Hansen and Robert J. Hodrick. Forward exchange rates as optimal predictors of future spot rates: An econometric analysis. *Journal of Political Economy*, 88(5):829–853, 1980. doi:10.1086/260910.

Lars Peter Hansen and Ravi Jagannathan. Implications of security market data for models of dynamic economies. *Journal of Political Economy*, 99(2):225–262, 1991. doi:10.1086/261749.

Fushing Hsieh and Bruce W. Turnbull. Nonparametric and semiparametric estimation of the receiver operating characteristic curve. *Annals of Statistics*, 24(1): 25–40, 1996. doi:10.1214/aos/1033066197.

Elton P. Hsu and S. R. Srinivasa Varadhan. *Probability Theory and Applications*. American Mathematical Society, 1999.

Jens Carsten Jackwerth. Recovering risk aversion from option prices and realized returns. *Review of Financial Studies*, 13(2):433–451, 2000. doi:10.1093/rfs/13.2.433.

Jens Carsten Jackwerth and Marco Menner. Does the Ross recovery theorem work empirically? *Journal of Financial Economics*, 137(3):723–739, 2020. doi:10.1016/j.jfineco.2020.03.006.

Roger Koenker and Gilbert Bassett. Regression quantiles. *Econometrica*, 46(1): 33–50, 1978. doi:10.2307/1913643.

Roger Koenker and José A. F. Machado. Goodness of fit and related inference processes for quantile regression. *Journal of the American Statistical Association*, 94(448):1296–1310, 1999. doi:10.1080/01621459.1999.10473882.

Erich L. Lehmann. Some concepts of dependence. *Annals of Mathematical Statistics*, 37(5):1137–1153, 1966. doi:10.1214/aoms/1177699260.

Matthew Linn, Sophie Shive, and Tyler Shumway. Pricing kernel monotonicity and conditional information. *Review of Financial Studies*, 31(2):493–531, 2018. doi:10.1093/rfs/hhx095.

Yan Liu. Index option returns and generalized entropy bounds. *Journal of Financial Economics*, 139(3):1015–1036, 2021. doi:10.1016/j.jfineco.2020.08.011.

Ian Martin. Consumption-based asset pricing with higher cumulants. *Review of Economic Studies*, 80(2):745–773, 2013. doi:10.1093/restud/rds029.

Ian Martin. What is the expected return on the market? *Quarterly Journal of Economics*, 132(1):367–433, 2017. doi:10.1093/qje/qjw034.

Ian Martin and Christian Wagner. What is the expected return on a stock? *Journal of Finance*, 74(4):1887–1929, 2019. doi:10.1111/jofi.12778.

Alexander J. McNeil, Rüdiger Frey, and Paul Embrechts. *Quantitative Risk Management: Concepts, Techniques and Tools*. Princeton University Press, 2015.

Dimitris N. Politis and Joseph P. Romano. The stationary bootstrap. *Journal of the American Statistical Association*, 89(428):1303–1313, 1994. doi:10.1080/01621459.1994.10476870.

Likuan Qin and Vadim Linetsky. Long-term risk: A martingale approach. *Econometrica*, 85(1):299–312, 2017. doi:10.3982/ECTA13438.

Likuan Qin, Vadim Linetsky, and Yutian Nie. Long forward probabilities, recovery, and the term structure of bond risk premiums. *Review of Financial Studies*, 31 (12):4863–4883, 2018. doi:10.1093/rfs/hhy042.

Thomas A. Rietz. The equity risk premium a solution. *Journal of Monetary Economics*, 22(1):117–131, 1988. doi:10.1016/0304-3932(88)90172-9.

Joshua V. Rosenberg and Robert F. Engle. Empirical pricing kernels. *Journal of Financial Economics*, 64(3):341–372, 2002. doi:10.1016/S0304-405X(02)00128-9.

Stephen A. Ross. *Neoclassical Finance*. Princeton University Press, 2005.

Stephen A. Ross. The recovery theorem. *Journal of Finance*, 70(2):615–648, 2015. doi:10.1111/jofi.12092.

Robert J. Serfling. *Approximation Theorems of Mathematical Statistics*. John Wiley & Sons, 2009.

Karl N. Snow. Diagnosing asset pricing models using the distribution of asset returns. *Journal of Finance*, 46(3):955–983, 1991. doi:10.1111/j.1540-6261.1991.tb03773.x.

Michael Stutzer. A Bayesian approach to diagnosis of asset pricing models. *Journal of Econometrics*, 68(2):367–397, 1995. doi:10.1016/0304-4076(94)01656-K.

Engin A. Sungur. Dependence information in parameterized copulas. *Communications in Statistics - Simulation and Computation*, 19(4):1339–1360, 1990. doi:10.1080/03610919008812920.

Aad W. van der Vaart. *Asymptotic Statistics*. Cambridge University Press, 2000.

Jessica A. Wachter. Can time-varying risk of rare disasters explain aggregate stock market volatility? *Journal of Finance*, 68(3):987–1035, 2013. doi:10.1111/jofi.12018.

Ivo Welch and Amit Goyal. A comprehensive look at the empirical performance of equity premium prediction. *Review of Financial Studies*, 21(4):1455–1508, 2008. doi:10.1093/rfs/hhm014.

A Proofs

This Section contains proofs and detailed calculations of results used in the main paper.

A.1 Proof of Proposition 3.1

Proof. By definition

$$\tau = \mathbb{P}_t(R_{m,t\to N} \leq Q_{t,\tau}) = \mathbb{P}_t\left(\exp\left(-\frac{1}{2}\sigma_t^2 N + \sigma_t\sqrt{N}Z_{t+N}\right) \leq \exp(-\mu N)Q_{t,\tau}\right).$$

Similarly

$$\tau = \widetilde{\mathbb{P}}_t(R_{m,t\to N} \leq \widetilde{Q}_{t,\tau}) = \widetilde{\mathbb{P}}_t\left(\exp\left(-\frac{1}{2}\sigma_t^2 N + \sigma_t\sqrt{N}Z_{t+N}\right) \leq \exp(-r_f N)\widetilde{Q}_{t,\tau}\right).$$

As a result

$$e^{(\mu-r_f)N}\widetilde{Q}_{t,\tau} = Q_{t,\tau}. \tag{A.1}$$

Recall that the quantile regression estimator is equivariant to reparametrization of design: for any 2×2 nonsingular matrix A, we have

$$\widehat{\beta}(\tau; R, XA) = A^{-1}\widehat{\beta}(\tau; R, X).$$

By (A.1),

$$X(\tau) = \widetilde{X}(\tau) \times \underbrace{\begin{bmatrix} 1 & 0 \\ 0 & e^{(\mu-r_f)N} \end{bmatrix}}_{:=A}.$$

Therefore

$$\widehat{\beta}(\tau; R, X(\tau)) = \widehat{\beta}(\tau; R, \widetilde{X}(\tau)A) = A^{-1}\widehat{\beta}(\tau; R, \widetilde{X}(\tau)).$$

Hence, the predicted quantile using the physical quantile regression (3.9) equals

$$\begin{aligned}[1 \quad Q_{T+1,\tau}(R_{T+2})]\ \widehat{\beta}(\tau; R, X(\tau)) &= [1 \quad Q_{T+1,\tau}(R_{T+2})]A^{-1}\ \widehat{\beta}(\tau; R, \widetilde{X}(\tau)) \\ &= [1 \quad \widetilde{Q}_{T+1,\tau}(R_{T+2})]\ \widehat{\beta}(\tau; R, \widetilde{X}(\tau)).\end{aligned}$$

This last expression is exactly (3.10). ■

A.2 Proof of Theorem 4.1

Proof. I suppress the dependence of the τ-quantile on R and write $\widetilde{Q}_\tau \coloneqq \widetilde{Q}_\tau(R)$. Starting from the definition of a risk-neutral quantile, I obtain

$$\begin{aligned}\tau &= \widetilde{\mathbb{P}}\left[R \leq \widetilde{Q}_\tau\right] = \widetilde{\mathbb{E}}\left[\mathbb{1}\left(R \leq \widetilde{Q}_\tau\right)\right] = R_f \mathbb{E}\left[M \mathbb{1}\left(R \leq \widetilde{Q}_\tau\right)\right] \\ &= R_f\left[\mathbb{COV}\left(M, \mathbb{1}\left(R \leq \widetilde{Q}_\tau\right)\right) + \mathbb{E}\left[M\right]\mathbb{E}\left[\mathbb{1}\left(R \leq \widetilde{Q}_\tau\right)\right]\right] \\ &= R_f \mathbb{COV}\left(M, \mathbb{1}\left(R \leq \widetilde{Q}_\tau\right)\right) + \underbrace{\mathbb{E}\left[\mathbb{1}\left(R \leq \widetilde{Q}_\tau\right)\right]}_{=\phi(\tau)}. \end{aligned} \tag{A.2}$$

Rearranging then yields

$$\frac{\tau - \phi(\tau)}{R_f} = \mathbb{COV}\left(M, \mathbb{1}\left(R \leq \widetilde{Q}_\tau\right)\right).$$

Using Cauchy-Schwarz renders the inequality

$$\begin{aligned}\frac{|\tau - \phi(\tau)|}{R_f} &\leq \sigma(M)\sigma\left(\mathbb{1}\left(R \leq \widetilde{Q}_\tau\right)\right) \\ \frac{|\tau - \phi(\tau)|}{\sigma\left(\mathbb{1}\left(R \leq \widetilde{Q}_\tau\right)\right) R_f} &\leq \sigma(M). \end{aligned} \tag{A.3}$$

Finally, since $\mathbb{1}\left(R \leq \widetilde{Q}_\tau\right)$ is a Bernoulli random variable, it follows that

$$\sigma\left(\mathbb{1}\left(R \leq \widetilde{Q}_\tau\right)\right) = \sqrt{\phi(\tau)(1-\phi(\tau))}. \tag{A.4}$$

Theorem 4.1 now follows after substituting (A.4) into (A.3). ∎

A.3 Jointly normal return and SDF

In this Section, I prove (4.6) and (4.5), when M and R are jointly normal. First I derive (4.6). The proof of the local bound in Theorem 4.1 gives the following identity

$$\frac{|\tau - \phi(\tau)|}{R_f} = \left|\mathbb{COV}\left(\mathbb{1}\left(R \leq \widetilde{Q}_\tau\right), M\right)\right|.$$

Standard SDF properties also yield the well known result

$$\frac{|\mathbb{E}(R) - R_f|}{R_f} = \left|\mathbb{COV}\left(R, M\right)\right|.$$

These results, combined with (4.5) prove (4.6), since

$$\frac{\text{HJ bound}}{\text{local bound}} = \frac{\frac{|\mathbb{E}[R]-R_f|}{\sigma_R R_f}}{\frac{|\tau-\phi(\tau)|}{\sqrt{\phi(\tau)(1-\phi(\tau))}R_f}} \overset{(4.5)}{=} \frac{\sqrt{\phi(\tau)(1-\phi(\tau))}}{\sigma_R f_R(\widetilde{Q}_\tau)},$$

where $f_R(\widetilde{Q}_\tau)$ is the marginal density of R.

It remains to prove (4.5). I make use of the following covariance identities, which are due to W. Hoeffding.

Lemma A.1 (Hoeffding)**.** *For any integrable random variable X and Z with marginal CDFs F_X, F_Z and joint CDF $F_{X,Z}$, it holds that*

$$\mathbb{COV}\left[\mathbb{1}\left(Z \leq z\right), X\right] = -\int_{-\infty}^{\infty} \left[F_{X,Z}(x,z) - F_X(x)F_Z(z)\right] \mathrm{d}x \tag{A.5}$$

$$\mathbb{COV}\left[Z, X\right] = -\int_{-\infty}^{\infty} \mathbb{COV}\left[\mathbb{1}\left(Z \leq z\right), X\right] \mathrm{d}z. \tag{A.6}$$

Proof. See Lehmann (1966). ∎

I also need a relation for the bivariate normal distribution. Suppose that X, Z are jointly normal with correlation ρ, mean μ_X, μ_Z and variance σ_X^2, σ_Z^2, then

$$\frac{\partial \Phi_2(x, z; \rho, \mu_X, \mu_Z, \sigma_X^2, \sigma_Z^2)}{\partial \rho} = \sigma_X \sigma_Z \phi_2(x, z; \rho, \mu_X, \mu_Z, \sigma_X^2, \sigma_Z^2), \tag{A.7}$$

where $\Phi_2(\cdot)$ denotes the bivariate normal CDF and $\phi_2(\cdot)$ denotes the bivariate normal PDF (Sungur, 1990). We can now prove a covariance identity for jointly normal random variables.

Proposition A.2. *Suppose R and M are jointly normal with correlation ρ, then*

$$-\mathbb{COV}\left[\mathbb{1}\left(R \leq x\right), M\right] = \phi_R(x) \cdot \mathbb{COV}\left[R, M\right], \tag{A.8}$$

where $\phi_R(\cdot)$ is the marginal density of R.

Proof. To lighten notation, I suppress the dependence on $\mu_R, \mu_M, \sigma_R^2, \sigma_M^2$ in the joint

CDF and PDF. We then have

$$\begin{aligned}-\mathbb{COV}\left[\mathbb{1}\left(R \leq x\right), M\right] &= \int_{-\infty}^{\infty} \Phi_2(x, m; \rho) - \Phi_2(x, m; 0)\, \mathrm{d}m \\ &= \int_{-\infty}^{\infty} \int_{0}^{\rho} \sigma_R \sigma_M \phi_2(x, m; y)\, \mathrm{d}y\, \mathrm{d}m \\ &= \sigma_R \sigma_M \rho \phi_R(x) = \mathbb{COV}\left[M, R\right] \phi_R(x),\end{aligned}$$

where, in the first line, I use (A.5) together with $F_R(r)F_M(m) = \Phi_2(r, m; 0)$, the second line follows from (A.7) and the third line follows from Fubini's theorem to swap the order of integration and $\int_{-\infty}^{\infty} \phi_2(x, m; y)\, \mathrm{d}m = \phi_R(x)$. ■

Remark. The second covariance identity in (A.6) shows that $\mathbb{COV}\left[\mathbb{1}\left(R \leq x\right), M\right]$ is a measure of local dependence. In case of joint normality (A.8), the weight is given by the marginal PDF. For other distributions, the weighting factor is more complicated, but sometimes can be given an explicit form using a *local Gaussian representation* (see Chernozhukov et al. (2018)).

A.4 Lognormal return and SDF

This Section provides a closed form approximation for the relative efficiency between the HJ and local bound under joint lognormality. The result depends on Stein's Lemma (Casella and Berger, 2002, Lemma 3.6.5):[26]

Lemma A.3 (Stein's Lemma)**.** *If X_1, X_2 are bivariate normal, $g : \mathbb{R} \to \mathbb{R}$ is differentiable and $\mathbb{E}\left|g'(X_1)\right| < \infty$, then*

$$\mathbb{COV}\left(g(X_1), X_2\right) = \mathbb{E}\left[g'(X_1)\right] \mathbb{COV}(X_1, X_2).$$

To prove the approximation, recall the distribution assumption

$$\begin{aligned}R &= e^{(\mu_R - \frac{\sigma_R^2}{2})\lambda + \sigma_R \sqrt{\lambda} Z_r} \\ M &= e^{-(r_f + \frac{\sigma_M^2}{2})\lambda + \sigma_M \sqrt{\lambda} Z_M}.\end{aligned}$$

Both Z_R and Z_M are standard normal random variables with correlation ρ. First, approximate M by a first order Taylor expansion, which gives

$$\widehat{M} = e^{-(r_f + \frac{\sigma_M^2}{2})\lambda} + Z_M \sigma_M \sqrt{\lambda} e^{-(r_f + \frac{\sigma_M^2}{2})\lambda}.$$

[26] I use the form of Stein's Lemma reported in Cochrane (2005, p. 163), which follows from Stein's lemma as reported in Casella and Berger (2002).

Notice that $\widehat{M} = M + o_p(\sqrt{\lambda})$. Consequently, by Stein's Lemma

$$\begin{aligned}
&\mathbb{COV}(R, M) \approx \mathbb{COV}(R, \widehat{M}) = \sigma_M \sqrt{\lambda} e^{-(r_f + \frac{\sigma_M^2}{2})\lambda} \mathbb{COV}(R, Z_M) \\
&= \sigma_M \sqrt{\lambda} e^{-(r_f + \frac{\sigma_M^2}{2})\lambda} \mathbb{E}\left[\sigma_R \sqrt{\lambda} \exp\left(\left[\mu_R - \frac{\sigma_R^2}{2}\right]\lambda + \sigma_R \sqrt{\lambda} Z_R\right)\right] \mathbb{COV}(Z_R, Z_M) \\
&= \sigma_M \sigma_R \lambda e^{-(r_f + \frac{\sigma_M^2}{2})\lambda} e^{\mu_R \lambda} \mathbb{COV}(Z_R, Z_M).
\end{aligned}$$

By Proposition A.2,

$$\begin{aligned}
&\mathbb{COV}(\mathbb{1}(\log R \le x), M) \approx \mathbb{COV}\left(\mathbb{1}(\log R \le x), \widehat{M}\right) \\
&= \sigma_M \sqrt{\lambda} e^{-(r_f + \frac{\sigma_M^2}{2})\lambda} \mathbb{COV}(\mathbb{1}(\log R \le x), Z_M) \\
&= \sigma_M \sqrt{\lambda} e^{-(r_f + \frac{\sigma_M^2}{2})\lambda} \mathbb{COV}\left(\mathbb{1}\left((\mu_R - \sigma_R^2/2)\lambda + \sigma_R \sqrt{\lambda} Z_R \le x\right), Z_M\right) \\
&= -\sigma_M \sqrt{\lambda} e^{-(r_f + \frac{\sigma_M^2}{2})\lambda} f(x) \mathbb{COV}(Z_R, Z_M).
\end{aligned}$$

Here, f is the density of a normal random variable with mean $(\mu_R - \sigma_R^2/2)\lambda$ and variance $\lambda\sigma_R^2$. As a result,

$$\left|\frac{\mathbb{E}[R] - e^{\lambda r_f}}{\tau - \phi(\tau)}\right| \approx \frac{\sigma_R \sqrt{\lambda} e^{\mu_R \lambda}}{f(x)}. \tag{A.9}$$

The same reasoning in Example 4.2 implies that the relative efficiency between the HJ and local bound can be approximated by

$$\frac{\text{HJ bound}}{\text{local bound}} = \frac{\frac{|\mathbb{E}[R] - R_f|}{\sigma(R) R_f}}{\frac{|\tau - \phi(\tau)|}{\sqrt{\phi(\tau)(1-\phi(\tau))} R_f}} \tag{A.10}$$

$$\overset{(A.9)}{\approx} \frac{\sqrt{\mathbb{P}(r \le x) \cdot (1 - \mathbb{P}(r \le x))}}{\sigma(R)} \times \frac{\sigma_R \sqrt{\lambda} e^{\mu_R \lambda}}{f(x)}, \tag{A.11}$$

where $r = \log R$ and $x = \log \widetilde{Q}_\tau$. Using the same reasoning as in Example 4.2, the expression on the right hand side of (A.10) is minimized by choosing $x = \log \widetilde{Q}_\tau^*$ s.t. $\mathbb{P}(R \le \widetilde{Q}_\tau^*) = 1/2$. In that case the relative efficiency equals

$$\frac{\sqrt{2\pi\sigma_R^2} \sqrt{\lambda} e^{\mu_R \lambda}}{2\sqrt{[\exp(\sigma_R^2 \lambda) - 1] \exp(2\mu_R \lambda)}} = \frac{1}{2} \sqrt{\frac{2\pi\sigma_R^2 \lambda}{\exp(\sigma_R^2 \lambda) - 1}}.$$

A.5 Local bound Pareto distribution

Proof of Proposition 4.2. (i) The distribution of returns is Pareto, since

$$\begin{aligned}\mathbb{P}(R \leq x) &= \mathbb{P}\left(U^{-\beta} \leq x/B\right) \\ &= \mathbb{P}\left(U \geq (x/B)^{-\frac{1}{\beta}}\right) = 1 - \left(\frac{x}{B}\right)^{-\frac{1}{\beta}}, \qquad x \geq B.\end{aligned}$$

(ii) Since $R_f M$ is the Radon-Nikodym derivative that induces a change of measure from $\mathbb{P}$ to $\widetilde{\mathbb{P}}$, it follows that

$$\begin{aligned}\widetilde{\mathbb{P}}(R \leq x) &= R_f \mathbb{E}\left[M \mathbb{1}\left(R \leq x\right)\right] \\ &= R_f \int_0^1 A u^\alpha \mathbb{1}\left(B u^{-\beta} \leq x\right) \mathrm{d}u \\ &= R_f A \int_0^1 u^\alpha \mathbb{1}\left(u \geq \left(\frac{x}{B}\right)^{-\frac{1}{\beta}}\right) \mathrm{d}u \\ &= \frac{R_f A}{\alpha+1}\left(1 - \left(\frac{x}{B}\right)^{-\frac{\alpha+1}{\beta}}\right) \\ &= 1 - \left(\frac{x}{B}\right)^{-\frac{\alpha+1}{\beta}}.\end{aligned}$$

The last line follows from (A.14) below.

(iii) Routine calculations show that the mean and variance of R are given by (provided $\beta < 1/2$)

$$\mathbb{E}\left[R\right] = \frac{B}{1-\beta} \qquad \sigma^2(R) = \frac{B^2}{1-2\beta} - \left(\frac{B}{1-\beta}\right)^2. \tag{A.12}$$

Likewise, the distribution of the SDF follows from

$$\mathbb{P}\left(M \leq x\right) = \mathbb{P}\left(A U^\alpha \leq x\right) = \left(\frac{x}{A}\right)^{\frac{1}{\alpha}}, \quad 0 \leq x \leq A.$$

In this case, M is said to have a Pareto lower tail. The expectation is given by

$$\mathbb{E}\left[M\right] = \frac{A}{\alpha+1}.$$

The constraint $\mathbb{E}\left[MR\right] = 1$ forces

$$\frac{AB}{\alpha - \beta + 1} = 1. \tag{A.13}$$

In addition from $\mathbb{E}[M] = \frac{1}{R_f}$ it follows

$$\frac{A}{\alpha+1} = \frac{1}{R_f}. \tag{A.14}$$

The Sharpe ratio can now be computed from (A.12) and (A.14).

(iv) It is straightforward to show that the quantiles of a **Par**(C, ζ) distribution are given by

$$Q_\tau = C \times (1-\tau)^{-1/\zeta}.$$

It therefore follows that the risk-neutral quantile function is equal to

$$\widetilde{Q}_\tau = B(1-\tau)^{-\frac{\beta}{\alpha+1}}.$$

As a result

$$\begin{aligned}\mathbb{P}(R \leq \widetilde{Q}_\tau) &= \mathbb{P}\left(R \leq B(1-\tau)^{-\frac{\beta}{\alpha+1}}\right) \\ &= 1 - \left(\frac{B}{B(1-\tau)^{\frac{-\beta}{\alpha+1}}}\right)^{\frac{1}{\beta}} \\ &= 1 - (1-\tau)^{\frac{1}{\alpha+1}}.\end{aligned}$$

Hence, the local bound evaluates to

$$\frac{1}{R_f}\frac{|\tau - \phi(\tau)|}{\sqrt{\phi(\tau)(1-\phi(\tau))}} = \frac{A}{1+\alpha}\frac{\left|\tau - 1 + (1-\tau)^{\frac{1}{\alpha+1}}\right|}{\sqrt{(1-(1-\tau)^{\frac{1}{\alpha+1}})(1-\tau)^{\frac{1}{\alpha+1}}}}.$$

(v) The HJ bound, as given by the Sharpe ratio in (4.10), goes to 0 as $\beta \uparrow 1/2$ since $\sigma(R) \uparrow \infty$.

■

A.6 Disaster risk probabilities

This section contains details about the disaster risk model in Figure 3. Let $F(\cdot)$ denote the CDF of Δc. Backus et al. (2011, p. 1976) show that

$$F(-b) = \sum_{j=0}^{\infty} \Phi\left(\frac{-b-\mu-j\theta}{\sqrt{\sigma^2+j\nu^2}}\right) \cdot \frac{e^{-\kappa}\kappa^j}{j!}, \tag{A.15}$$

where $\Phi(\cdot)$ is the CDF of a standard normal distribution. From here it is straightforward to compute the physical CDF of return on equity, $R = \exp(\lambda \Delta c)$, by a change of variables and truncating the sum in (A.15). Secondly, to obtain the risk-

neutral CDF, I use the result of Backus et al. (2011, p. 1987) that the risk-neutral distribution of Δc is the same as in (A.15), with new parameters

$$\widetilde{\kappa} = \kappa e^{-\gamma\theta+(\gamma\nu)^2/2}, \quad \widetilde{\theta} = \theta - \gamma\nu^2.$$

It follows that $\widetilde{\kappa} > \kappa$ if $\theta < 0$ (more jumps) and $\widetilde{\theta} < \theta$ (outcomes of jump is more negative on average). This explains the fat left tail of the risk-neutral distribution in Figure 3. The local bound, HJ bound and SDF volatility can now easily be calculated from the expression for the physical and risk-neutral distribution.

A.7 Derivation of Gâteaux derivative

In this Section I derive (6.3). For ease of exposition, I drop the time subscripts. For $\lambda \in [0,1]$, define $\widetilde{F}_\lambda := (1-\lambda)\widetilde{F} + \lambda F$. The following (trivial) identity will prove helpful[27]

$$\tau = \widetilde{F}_\lambda \widetilde{F}_\lambda^{-1}. \tag{A.16}$$

To further simplify notation, write $q(\lambda) := \widetilde{F}_\lambda^{-1}$. Then (A.16) becomes

$$\tau = (1-\lambda)\widetilde{F}(q(\lambda)) + \lambda F(q(\lambda)).$$

Applying the implicit function theorem, we obtain

$$q'(\lambda) = -\frac{-\widetilde{F}(q(\lambda)) + F(q(\lambda))}{(1-\lambda)\widetilde{f}(q(\lambda)) + \lambda f(q(\lambda))}.$$

Plug in $\lambda = 0$ to get

$$q'(0) = -\frac{-\widetilde{F}(q(0)) + F(q(0))}{\widetilde{f}(q(0))}. \tag{A.17}$$

Notice that

$$\widetilde{F}_\lambda\big|_{\lambda=0} = \widetilde{F} \implies q(\lambda)\big|_{\lambda=0} = q(0) = \widetilde{F}^{-1}. \tag{A.18}$$

Substitute (A.18) into (A.17) to obtain

$$q'(0) = -\frac{-\widetilde{F}(\widetilde{F}^{-1}) + F(\widetilde{F}^{-1})}{\widetilde{f}(\widetilde{F}^{-1})} = \frac{\tau - F(\widetilde{F}^{-1})}{\widetilde{f}(\widetilde{F}^{-1})}. \tag{A.19}$$

Notice that $q'(0)$ is exactly equal to the Gâteaux derivative from the definition in (6.2), since

$$\frac{\partial}{\partial\lambda}\varphi\left[(1-\lambda)\widetilde{F} + \lambda F\right]\Big|_{\lambda=0} = \frac{\partial}{\partial\lambda} q(\lambda)\Big|_{\lambda=0} = q'(0).$$

[27] This "equality" may actually only be an inequality for some τ, but this is immaterial to the argument.

A.8 Proof of Theorem 6.3 and Corollary 6.4

Before I prove Theorem 6.3 and Corollary 6.4, I collect several results about the SDF in representative agent models.

Lemma A.4. *Assume a representative agent model with SDF given by (6.5), then*

$$\tau - F_t(\widetilde{Q}_{t,\tau}) = -\frac{\widetilde{\mathbb{COV}}_t\left[\mathbb{1}\left(R_{m,t\to N} \leq \widetilde{Q}_{t,\tau}\right), \zeta(R_{m,t\to N})\right]}{\widetilde{\mathbb{E}}_t\left[\zeta(R_{m,t\to N})\right]}, \tag{A.20}$$

where $\zeta(\cdot)$ is defined in (6.6).

Proof. Use the reciprocal of the SDF to pass from physical to risk-neutral measure

$$\begin{aligned} F_t(\widetilde{Q}_{t,\tau}) &= \mathbb{E}_t\left[\mathbb{1}\left(R_{m,t\to N} \leq \widetilde{Q}_{t,\tau}\right)\right] = \widetilde{\mathbb{E}}_t\left[\mathbb{1}\left(R_{m,t\to N} \leq \widetilde{Q}_{t,\tau}\right)\frac{\mathbb{E}_t\left[M_{t\to N}\right]}{M_{t\to N}}\right] \\ &= \widetilde{\mathbb{COV}}_t\left[\mathbb{1}\left(R_{m,t\to N} \leq \widetilde{Q}_{t,\tau}\right), \frac{\mathbb{E}_t\left[M_{t\to N}\right]}{M_{t\to N}}\right] + \tau. \end{aligned} \tag{A.21}$$

Rearranging the above and using the definition of $\zeta(\cdot)$, as well as (6.5), we obtain (A.20). ∎

Before I proceed, recall the definition of G in Assumption 6.2:

$$G(x) = \frac{(x - R_{f,t\to N})^4}{4!}\int_0^1 \zeta^{(4)}(R_{f,t\to N} + s(x - R_{f,t\to N}))\,(1-s)^3\,\mathrm{d}s.$$

Under Assumption 6.2, it follows that $G(x) \leq 0$ and I use this fact in Lemma A.7 below. In the proofs that follow, I repeatedly use Taylor's theorem with integral remainder, which I state for completeness.

Lemma A.5 (Taylor's theorem)**.** *Let $\zeta^{(3)}(\cdot)$ be absolutely continuous on the closed interval between a and x, then*

$$\zeta(x) = \sum_{k=0}^{3}\frac{\zeta^{(k)}(a)}{k!}(x-a)^k + \int_a^x \frac{\zeta^{(4)}(t)}{4!}(x-t)^3\,\mathrm{d}t.$$

Lemma A.6. *Under Assumption 6.2,*

$$\widetilde{\mathbb{E}}_t\left[\zeta(R_{m,t\to N})\right] \leq \sum_{k=0}^{3}\theta_k\widetilde{\mathbb{M}}_{t\to N}^{(k)} = 1 + \sum_{k=1}^{3}\theta_k\widetilde{\mathbb{M}}_{t\to N}^{(k)}.$$

Proof. In the integral of Lemma A.5, substitute $s = (t-a)/(x-a)$ to get

$$\begin{aligned}\zeta(x) &= \sum_{k=0}^{3} \frac{\zeta^{(k)}(a)}{k!}(x-a)^k + (x-a)^4 \int_0^1 \frac{\zeta^{(4)}(a+s(x-a))}{4!}(1-s)^3 \, \mathrm{d}s \\ &\leq \sum_{k=0}^{3} \frac{\zeta^{(k)}(a)}{k!}(x-a)^k,\end{aligned}$$

since $\zeta^{(4)}(x) < 0$ by Assumption 6.2. Using this result and taking expectations, we obtain

$$\widetilde{\mathbb{E}}_t \left[\zeta(R_{m,t\to N})\right] \leq \sum_{k=0}^{3} \theta_k \widetilde{\mathbb{M}}^{(k)}_{t\to N}.$$

■

I now prove Theorem 6.3 and Corollary 6.4.

Proof of Theorem 6.3 and Corollary 6.4. By Taylor's theorem A.5,

$$\begin{aligned}&-\widetilde{\mathbb{COV}}_{\mathrm{t}}\left[\mathbb{1}\left(R_{m,t\to N} \leq \widetilde{Q}_{t,\tau}\right), \zeta(R_{m,t\to N})\right] = \\ &\sum_{k=1}^{3} \theta_k \left(\tau \widetilde{\mathbb{M}}^{(k)}_{t\to N} - \widetilde{\mathbb{M}}^{(k)}_{t\to N}[\widetilde{Q}_{t,\tau}]\right) - \widetilde{\mathbb{COV}}_{\mathrm{t}}\left[\mathbb{1}\left(R_{m,t\to N} \leq \widetilde{Q}_{t,\tau}\right), G(R_{m,t\to N})\right] \\ &\geq \sum_{k=1}^{3} \theta_k \left(\tau \widetilde{\mathbb{M}}^{(k)}_{t\to N} - \widetilde{\mathbb{M}}^{(k)}_{t\to N}[\widetilde{Q}_{t,\tau}]\right).\end{aligned} \tag{A.22}$$

The last line follows from Lemma A.7 below. Hence,

$$\begin{aligned}\tau - F_t(\widetilde{Q}_{t,\tau}) &= -\frac{\widetilde{\mathbb{COV}}_{\mathrm{t}}\left[\mathbb{1}\left(R_{m,t\to N} \leq \widetilde{Q}_{t,\tau}\right), \zeta(R_{m,t\to N})\right]}{\widetilde{\mathbb{E}}_t\left[\zeta(R_{m,t\to N})\right]} \\ &\geq \frac{\sum_{k=1}^{3} \theta_k \left(\tau \widetilde{\mathbb{M}}^{(k)}_{t\to N} - \widetilde{\mathbb{M}}^{(k)}_{t\to N}[\widetilde{Q}_{t,\tau}]\right)}{1 + \sum_{k=1}^{3} \theta_k \widetilde{\mathbb{M}}^{(k)}_{t\to N}},\end{aligned}$$

where the first identity follows from Lemma A.4 and the inequality follows from (A.22) and Lemma A.6. Therefore,

$$\begin{aligned}Q_{t,\tau} - \widetilde{Q}_{t,\tau} &\overset{(6.4)}{\approx} \frac{\tau - F_t(\widetilde{Q}_{t,\tau})}{\widetilde{f}_t(\widetilde{Q}_{t,\tau})} \\ &\geq \frac{1}{\widetilde{f}_t(\widetilde{Q}_{t,\tau})} \left(\frac{\sum_{k=1}^{3} \theta_k \left(\tau \widetilde{\mathbb{M}}^{(k)}_{t\to N} - \widetilde{\mathbb{M}}^{(k)}_{t\to N}[\widetilde{Q}_{t,\tau}]\right)}{1 + \sum_{k=1}^{3} \theta_k \widetilde{\mathbb{M}}^{(k)}_{t\to N}}\right).\end{aligned} \tag{A.23}$$

If additionally (6.10) holds, then

$$\theta_1 = \frac{1}{R_{f,t\to N}}, \theta_2 = -\frac{1}{R_{f,t\to N}^2}, \text{ and } \theta_3 = \frac{1}{R_{f,t\to N}^3}.$$

Using this in (A.23) gives

$$Q_{t,\tau} - \widetilde{Q}_{t,\tau} \geq \frac{1}{\widetilde{f}_t(\widetilde{Q}_{t,\tau})} \left(\frac{\sum_{k=1}^3 \frac{(-1)^{k+1}}{R_{f,t\to N}^k} \left(\tau \widetilde{\mathbb{M}}_{t\to N}^{(k)} - \widetilde{\mathbb{M}}_{t\to N}^{(k)}[\widetilde{Q}_{t,\tau}] \right)}{1 + \sum_{k=1}^3 \frac{(-1)^{k+1}}{R_{f,t\to N}^k} \widetilde{\mathbb{M}}_{t\to N}^{(k)}} \right).$$

■

Lemma A.7. *Suppose that Assumption 6.2. In addition, define τ^* so that $G(\widetilde{Q}_{t,\tau^*}) = G(R_{m,t\to N})$. Then for all $\tau \leq \tau^*$,*

$$\widetilde{\mathbb{COV}}_t \left[\mathbb{1}\left(R_{m,t\to N} \leq \widetilde{Q}_{t,\tau} \right), G(R_{m,t\to N}) \right] \leq 0. \tag{A.24}$$

Proof. If $\zeta^{(4)} \equiv 0$, then (A.24) trivially holds for all τ. Hence, assume that $\zeta^{(4)}$ is not identically equal to zero. Rewrite the covariance in (A.24) as

$$\Gamma(\tau) = \widetilde{\mathbb{E}}_t \left[\left(\mathbb{1}\left(R_{m,t\to N} \leq \widetilde{Q}_{t,\tau} \right) - \tau \right) G(R_{m,t\to N}) \right].$$

Notice that $\Gamma(\tau) \to 0$ as $\tau \to 0$ due to the Cauchy-Schwarz inequality and $\mathbb{1}(R_{m,t\to N} \leq \widetilde{Q}_{t,\tau})$ is Bernoulli with variance $\tau(1-\tau)$. Differentiate with respect to τ and using Leibniz' rule, I get

$$\Gamma'(\tau) = G(\widetilde{Q}_{t,\tau}) - \underbrace{\widetilde{\mathbb{E}}_t \left[G(R_{m,t\to N}) \right]}_{<0}. \tag{A.25}$$

The right most term is negative due to Assumption 6.2. Define τ^* as the smallest $\tau > 0$ such that $\Gamma'(\tau^*) = 0$. Notice that we can always find such a number, since the right most term in (A.25) is independent of τ, while the first term on the right goes to some number smaller than $\widetilde{\mathbb{E}}_t \left[G(R_{m,t\to N}) \right]$ (by (6.7)) and $G(\widetilde{Q}_{t,\tau_1}) = 0$ if $\widetilde{Q}_{t,\tau_1} = R_{f,t\to N}$. Hence, by the intermediate value theorem there exists a $\tau^* > 0$ such that $\Gamma(\tau^*) = 0$. ■

A.8.1 Verifying the assumptions in representative agent models

The proof of Theorem 6.3 relies on Assumption 6.2. I verify that this Assumption holds for log and CRRA utility, but not for CARA utility.

A.8.2 Log utility

In this case $u(x) = \log x$. It follows that $\zeta(x) = x/R_{f,t\to N}$. Clearly $\zeta^{(4)}(x) = 0$ and Assumption 6.2 holds.

A.8.3 CRRA utility

In this case, $u(x) = \frac{x^{1-\gamma}}{1-\gamma}$ and assume $\gamma > 1$. It follows that $\zeta(x) = (\frac{x}{R_{f,t\to N}})^{\gamma}$ and hence

$$\zeta^{(4)}(x) = \frac{1}{R_{f,t\to N}^{\gamma}}\gamma(\gamma-1)(\gamma-2)(\gamma-3)x^{\gamma-4}.$$

Part (ii) of Assumption 6.2 holds if $\gamma \in (0,1)$. Part (iii) further restricts the risk-aversion coefficient. To see this, observe that the integral in (6.7) is proportional to

$$-\int_0^1 (1-s)^{\gamma-1}\,\mathrm{d}s.$$

This integral goes to $-\infty$ the closer γ gets to 1. Hence, if γ is sufficiently close to 1, condition (iii) holds and if $\gamma = 1$ we recover the log utility case.

A.8.4 CARA utility

In this case, $u(x) = 1 - e^{-\gamma x}$ and $\zeta(x) = e^{\gamma^*(x - R_{f,t\to N})}$, where $\gamma^* = W_t\gamma$. Since $\zeta^{(4)} > 0$, Assumption 6.2 does not hold.

A.9 Formulas for market moments

This Section presents formulas for the (un)truncated risk-neutral moments of the excess market return. I use a slight abuse of notation and write $\widetilde{Q}(\tau) \coloneqq \widetilde{Q}_\tau(R_{m,t\to N})$, to emphasize that the integrals below are taken with respect to τ.

Proposition A.8. *Any risk-neutral moment can be computed from the risk-neutral quantile function, since*

$$\widetilde{\mathbb{E}}_t\left[(R_{m,t\to N} - R_{f,t\to N})^n\right] = \int_0^1 [\widetilde{Q}_\tau(R_{m,t\to N} - R_{f,t\to N})]^n\,\mathrm{d}\tau = \int_0^1 [\widetilde{Q}(\tau) - R_{f,t\to N}]^n\,\mathrm{d}\tau. \tag{A.26}$$

Moreover, any truncated risk-neutral moment can be calculated by

$$\widetilde{\mathbb{E}}_t\left[(R_{m,t\to N} - R_{f,t\to N})^n \mathbb{1}\left(R_{m,t\to N} \le k_0\right)\right] = \int_0^{\widetilde{F}_t(k_0)} [\widetilde{Q}(\tau) - R_{f,t\to N}]^n\,\mathrm{d}\tau.$$

Remark. Frequently I use $k_0 = \widetilde{Q}_\tau$, in which case the truncated moment formula reduces to

$$\widetilde{\mathbb{E}}_t\left[(R_{m,t\to N} - R_{f,t\to N})^n \mathbb{1}\left(R_{m,t\to N} \le \widetilde{Q}_\tau\right)\right] = \int_0^{\tau} [\widetilde{Q}(p) - R_{f,t\to N}]^n\,\mathrm{d}p.$$

Proof. For any random variable X and integer n such that the n-th moment exists, we have

$$\mathbb{E}\left[X^n\right] = \int_0^1 \left[Q_X(\tau)\right]^n \mathrm{d}\tau.$$

This follows straightforward from the substitution $x = Q(\tau)$. Now use that for any constant $a \in \mathbb{R}$, $Q_{X-a}(\tau) = Q_X(\tau) - a$ to derive (A.26). The truncated formula follows similarly. ■

B Estimating the risk-neutral quantile function

B.1 Data description

To estimate the risk-neutral quantile curve for each point in time, I use daily option prices from OptionMetrics covering the period 01-01-1996 until 12-31-2021. This consists of European Put and Call option data on the S&P 500 index. The option contract further contains information on the highest closing bid and lowest closing ask price and price of the forward contract on the underlying security. I use the mid-point of the bid and ask price to proxy for the unobserved option price. In addition, I obtain data on the daily risk-free rate from Kenneth French' website.[28] Finally, I obtain stock price data on the closing price of the S&P 500 from WRDS.

I use an additional cleaning procedure for the option data, prior to estimating the martingale measure. All observations are dropped for which the highest closing bid price equals zero, as well as all option prices that violate no-arbitrage bounds. Subsequently, I drop all option prices with maturity less than 7 days or greater than 500 days. After the cleaning procedure, I'm left with 23,264,113 option-day observations.

I discard all observations prior to 2003 for the quantile regression application, since there are many days in the period 1996-2003 that have insufficient option data to estimate $\widetilde{Q}_{t,\tau}$ at the 30, 60 and 90-day horizon. Occasionally it happens that I cannot estimate the risk-neutral quantile on a specific day in the post 2003 period and I discard these days as well.[29]

B.2 Estimating the risk-neutral quantile function

There is a substantial literature on how to extract the martingale measure from option prices. I use the *RND Fitting Tool* application on MATLAB, which is developed

[28] See http://mba.tuck.dartmouth.edu/pages/faculty/ken.french/data_library.html#Research

[29] The number of days I cannot estimate the risk-neutral PDF is very small, about 2% in total. Most of these days occur at the beginning of the sample period.

by Barletta and Santucci de Magistris (2018).[30]. The tool is based on the orthogonal polynomial expansion of Filipović et al. (2013). In short, the idea is to approximate the conditional risk-neutral density function by an expansion of the form

$$\widetilde{f}_t(x) \approx \phi(x) \left[1 + \sum_{k=1}^{K} \sum_{i=0}^{k} c_k w_{i,k} x^k \right],$$

where $\phi(x)$ is an arbitrary density and the polynomial term serves to tilt the density function towards the risk-neutral distribution. Further details about the estimation of the coefficients $w_{i,k}$ and c_k can be found in Filipović et al. (2013).

For my purpose, I need to choose the kernel function $\phi(\cdot)$, the estimation method for c_k and the degree of the expansion K. I follow the recommendation of Barletta and Santucci de Magistris (2018) and use the *double beta* distribution for the kernel and principal component analysis to estimate c_k. This is the most robust method for S&P500 options. To avoid overfitting, I use $K = 3$ if the number of option data is less than 70, $K = 6$ if the number is less than 100 and $K = 8$ otherwise. This choice renders a good approximation for most time periods.

I interpolate the estimated risk-neutral densities for a given time period. Occasionally, there are no two interpolation points. In such cases, I drop the observations to avoid negative density estimates due to extrapolation. Since the RND Fitting Tool is designed for an equal number of put and call options, I use Put-Call parity to convert in-the-money call prices to put prices and vice versa. Subsequently, I use Black-Scholes implied volatilities to interpolate the Call-Put option price curve near the forward price. This transformation ensures that the risk-neutral density does not have a discontinuity for strike prices that are close to being at-the-money (Figlewski, 2010). Finally, I integrate the density function and take the inverse to obtain the risk-neutral quantile curve

$$\widetilde{Q}_{t,\tau} \coloneqq \inf \left\{ x \in \mathbb{R} : \tau \leq \widetilde{F}_t(x) \right\}, \quad \text{where } \widetilde{F}_t(x) = \int_0^x \widetilde{f}_t(y)\, \mathrm{d}y.$$

C Crash probability in representative agent models

In this Section, I derive several results about disaster probabilities in representative agent models.

[30]The application can be downloaded from the author's GITHUB page: https://github.com/abarletta/rndfittool

C.1 Crash probability with log utility

Chabi-Yo and Loudis (2020, Remark 1) show that their bounds on the equity premium equal the bounds of Martin (2017) when the representative agent has log preferences. Here, I derive the analogous result for the subjective crash probability of a log investor reported by Martin (2017, Result 2). In our notation, Martin (2017) shows that

$$\mathbb{P}_t\left(R_{m,t\to N} < \alpha\right) = \alpha\left[\mathrm{Put}_t'(\alpha S_t) - \frac{\mathrm{Put}_t(\alpha S_t)}{\alpha S_t}\right], \tag{C.1}$$

where Put_t' is the derivative of the put option price curve seen as a function of the strike. Under log preferences and using (A.21), it follows that

$$\begin{aligned}
&\mathbb{P}_t(R_{m,t\to N} < \widetilde{Q}_{t,\tau}) = \tau + \frac{1}{R_{f,t\to N}}\widetilde{\mathbb{COV}}_t\left[\mathbb{1}\left(R_{m,t\to N} \le \widetilde{Q}_{t,\tau}\right), R_{m,t\to N}\right] \\
&= \tau + \frac{1}{R_{f,t\to N}}\left(\widetilde{\mathbb{E}}_t\left[\mathbb{1}\left(R_{m,t\to N} \le \widetilde{Q}_{t,\tau}\right)R_{m,t\to N}\right] - \widetilde{\mathbb{E}}_t(R_{m,t\to N})\widetilde{\mathbb{E}}_t\left(\mathbb{1}\left(R_{m,t\to N} \le \widetilde{Q}_{t,\tau}\right)\right)\right) \\
&= \frac{1}{R_{f,t\to N}}\widetilde{\mathbb{E}}_t\left[\mathbb{1}\left(R_{m,t\to N} \le \widetilde{Q}_{t,\tau}\right)R_{m,t\to N}\right].
\end{aligned} \tag{C.2}$$

The result now follows upon substituting $\widetilde{Q}_\tau = \alpha$, since Martin (2017) shows that (C.2) equals the right hand side of (C.1).

C.2 Crash probability with CRRA utility

I now consider the case in which the representative agent has constant relative risk aversion (CRRA) utility, $u(x) = x^{1-\gamma}/(1-\gamma)$, where γ is the relative risk aversion parameter. First, I show that the excess market return is non-decreasing in γ *regardless* of the distribution of the market return.[31] The proof uses the following lemma, which is a special case of the FKG inequality (Hsu and Varadhan, 1999, Theorem 1.3).

Lemma C.1 (Chebyshev sum inequality)**.** *Let X be a random variable and let g, h both be non-increasing or non-decreasing. Then,*

$$\mathbb{E}\left(g(X)h(X)\right) \ge \mathbb{E}\left(g(X)\right)\mathbb{E}\left(h(X)\right).$$

The inequality is reversed if one is non-increasing and the other is non-decreasing.

Proof. Let X_1, X_2 be IID copies of X and assume that g, h are non-decreasing. It follows that

$$\left(g(X_1) - g(X_2)\right)\left(h(X_1) - h(X_2)\right) \ge 0. \tag{C.3}$$

Taking expectations on both sides completes the proof. The same proof goes through

[31] Cochrane (2005) derives this result when the distribution is lognormal.

if g, h are non-increasing. If one is non-increasing and the other is non-decreasing, then the inequality in (C.3) is reversed. ■

Proposition C.2. *Assume that a representative investor has CRRA utility, with* $\gamma \geq 0$ *and* $\mathbb{E}_t\left[R_{m,t\to N}^{\gamma+1} \log R_{m,t\to N}\right] < \infty$. *Then,* $\mathbb{E}_t\left[R_{m,t\to N}\right] - R_{f,t\to N}$, *is non-decreasing in* γ.

Proof. According to Chabi-Yo and Loudis (2020, Equation (53)), we have

$$\mathbb{E}_t\left[R_{m,t\to N}\right] - R_{f,t\to N} = \frac{\widetilde{\mathbb{E}}_t\left[R_{m,t\to N}^{\gamma+1}\right]}{\widetilde{\mathbb{E}}_t\left[R_{m,t\to N}^{\gamma}\right]} - R_{f,t\to N} =: g(\gamma).$$

It is enough to show that $g'(\gamma) \geq 0$ for $\gamma \geq 0$. Taking first order conditions, we need to show that

$$\widetilde{\mathbb{E}}_t\left[R_{m,t\to N}^{\gamma+1} \log R_{m,t\to N}\right] \widetilde{\mathbb{E}}_t\left[R_{m,t\to N}^{\gamma}\right] \geq \widetilde{\mathbb{E}}_t\left[R_{m,t\to N}^{\gamma+1}\right] \widetilde{\mathbb{E}}_t\left[R_{m,t\to N}^{\gamma} \log R_{m,t\to N}\right]. \tag{C.4}$$

Introduce another probability measure $\mathbb{P}^*$, defined as

$$\mathbb{E}_t^*\left[Z\right] \coloneqq \frac{\widetilde{\mathbb{E}}_t\left[Z R_{m,t\to N}^{\gamma}\right]}{\widetilde{\mathbb{E}}_t\left[R_{m,t\to N}^{\gamma}\right]}. \tag{C.5}$$

We can rewrite (C.4) into

$$\mathbb{E}_t^*\left[R_{m,t\to N}^{\gamma} \log R_{m,t\to N}\right] \geq \mathbb{E}_t^*\left[R_{m,t\to N}^{\gamma}\right] \mathbb{E}_t^*\left[\log R_{m,t\to N}\right]. \tag{C.6}$$

Inequality (C.6) follows from Lemma C.1. ■

I mimic the steps above to show that the physical distribution differs more from the risk-neutral distribution at every point in the support, whenever risk aversion is increasing.

Proposition C.3. *Assume that a representative investor has CRRA utility, with* $\gamma \geq 0$ *and* $\mathbb{E}_t\left[R_{m,t\to N}^{\gamma} \log R_{m,t\to N}\right] < \infty$, *then* $F_t(x)$ *is non-increasing in* γ. *In particular,* $\tau - F_t(\widetilde{Q}_{t,\tau})$ *is non-decreasing in* γ.

Proof. I start from the relation

$$F_t(x) = \widetilde{\mathbb{E}}_t\left[\frac{R_{m,t\to N}^{\gamma}}{\widetilde{\mathbb{E}}_t\left[R_{m,t\to N}^{\gamma}\right]} \mathbb{1}\left(R_{m,t\to N} \leq x\right)\right].$$

From first order conditions, we need to show that

$$\widetilde{\mathbb{E}}_t\left[\log(R_{m,t\to N})\mathbb{1}\left(R_{m,t\to N}\leq x\right)R_{m,t\to N}^{\gamma}\right]\widetilde{\mathbb{E}}_t\left[R_{m,t\to N}^{\gamma}\right]\leq \\ \widetilde{\mathbb{E}}_t\left[R_{m,t\to N}^{\gamma}\mathbb{1}\left(R_{m,t\to N}\leq x\right)\right]\widetilde{\mathbb{E}}_t\left[\log(R_{m,t\to N})R_{m,t\to N}^{\gamma}\right].$$

Using the same change of measure as in (C.5), we obtain the equivalent statement

$$\mathbb{E}_t^*\left[\log(R_{m,t\to N})\mathbb{1}\left(R_{m,t\to N}\leq x\right)\right]\leq\mathbb{E}_t^*\left[\mathbb{1}\left(R_{m,t\to N}\leq x\right)\right]\mathbb{E}_t^*\left[\log R_{m,t\to N}\right].$$

This inequality holds, since $\log(x)$ and $\mathbb{1}\left(x\leq x\right)$ are respectively increasing and non-increasing, hence the result follows from Lemma C.1. Using the substitution $x\to\widetilde{Q}_{t,\tau}$, it follows that $\tau-F_t(\widetilde{Q}_{t,\tau})$, is non-decreasing in γ. ■

Panel (a) in Figure C1 shows that the lower bound in the CRRA model is tight when $\gamma=1$, but it is rather conservative for $\gamma=3$. The influence of the lower bound on the quantile function is shown in Panel (b). The quantile approximation is accurate when $\gamma=1$, but once more conservative when $\gamma=3$. In both cases the risk-adjustment term uniformly improves upon the risk-neutral approximation.

C.3 Exponential utility

Here, I assume that the representative agent has exponential utility, $u(x)=1-e^{-\gamma^* x}$, where γ^* is the absolute risk aversion. According to Chabi-Yo and Loudis (2020, Equation (55)), the following expression for the equity premium obtains

$$\mathbb{E}_t\left[R_{m,t\to N}\right]-R_{f,t\to N}=\frac{\widetilde{\mathbb{E}}_t\left[R_{m,t\to N}e^{\gamma R_{m,t\to N}}\right]}{\widetilde{\mathbb{E}}_t\left[e^{\gamma R_{m,t\to N}}\right]}-R_{f,t\to N},$$

where $\gamma=\gamma^* W_t$ is relative risk aversion and W_t represents the agent's wealth at time t. Since there is a one-to-one relation between γ and γ^*, it follows from the results in Section C.2 that the equity premium is increasing in γ^* and so is the distance between the physical and risk-neutral distribution, as measured by: $\tau-F_t(\widetilde{Q}_{t,\tau})$.

D Other SDF bounds

In this Section, I analyze SDF bounds other than the one from Hansen and Jagannathan (1991). For each SDF bound, it is well known under which conditions they are tight. For example, the log bound of Bansal and Lehmann (1997) is known to bind for the growth-optimal portfolio. Under some conditions, the growth-optimal return is equal to the market return. Hence, an approach similar to Section 5.2 can be used to analyze if the market return is growth-optimal. Throughout, I repeatedly

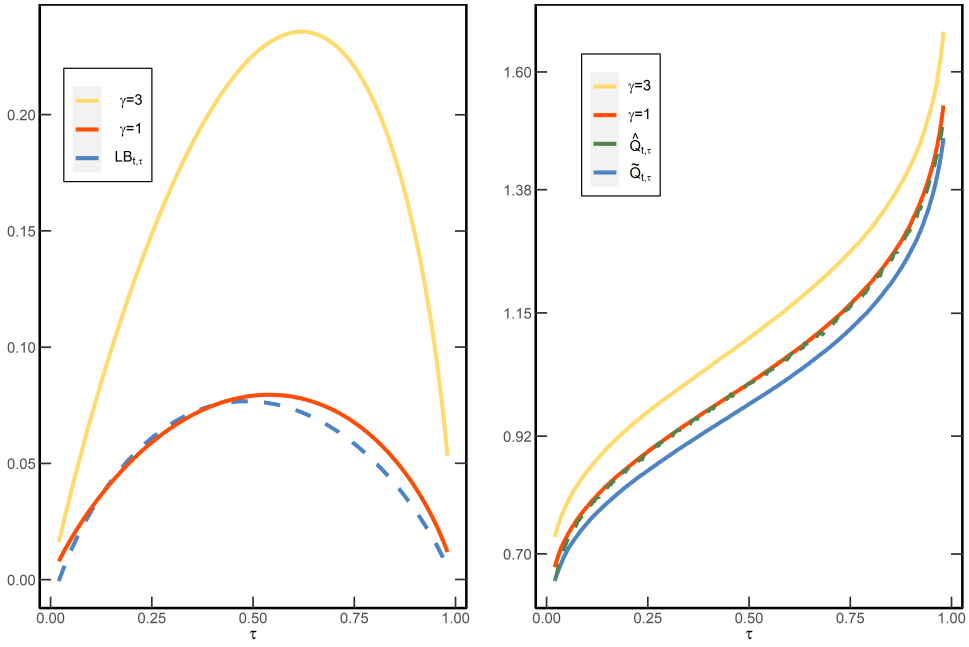

(a) Lower bound (b) Quantile function

Figure C1: **Lower bound with CRRA utility**. This figure shows the lower bound in a representative agent model with CRRA utility function, $u(x) = x^{1-\gamma}/(1-\gamma)$, for annual returns. The left panel shows $\text{LB}_{t,\tau}$ and the true risk-adjustment, $\tau - F_t(\widetilde{Q}_{t,\tau})$, for the risk aversion coefficient $\gamma \in \{1, 3\}$. The right panel shows the physical quantile function for $\gamma \in \{1, 3\}$, as well as the proxy for the physical quantile function, $\widehat{Q}_{t,\tau} = \widetilde{Q}_{t,\tau} + \text{RA}_{t,\tau}$, and the risk-neutral quantile function, $\widetilde{Q}_{t,\tau}$. The risk-neutral distribution is $\textbf{Logn}\left[(r - \frac{1}{2}\sigma^2)T, \sigma\sqrt{T}\right]$, where $r = 0, \sigma = 0.2$ and $T = 1$.

use the following identity derived in the proof of the local bound

$$\tau = R_f \mathbb{E}\left[M \mathbb{1}\left(R \leq \widetilde{Q}_\tau\right)\right]. \tag{D.1}$$

D.1 Bound of Snow (1991)

Snow (1991) derives a continuum of bounds of higher order moments on the SDF. In somewhat simplified form, the idea is to use Hölder's inequality to the defining SDF equation

$$1 = \mathbb{E}\left[MR\right] \leq \mathbb{E}\left[M^p\right]^{\frac{1}{p}} \mathbb{E}\left[R^q\right]^{\frac{1}{q}},$$

for Hölder exponents $\frac{1}{p} + \frac{1}{q} = 1$ and $p > 1$. Rearranging gives the restriction on the p-th norm of the SDF

$$\mathbb{E}\left[M^p\right]^{\frac{1}{p}} \geq \mathbb{E}\left[R^q\right]^{-\frac{1}{q}}.$$

The quantile relation (D.1) can similarly be exploited by applying Hölder's inequality on the right hand side, which gives

$$\mathbb{E}\left[M^p\right]^{\frac{1}{p}} \geq \left(\frac{\tau}{R_f}\right) \mathbb{E}\left[\mathbb{1}\left(R \leq \widetilde{Q}_\tau\right)\right]^{-\frac{1}{q}}.$$

D.2 Bound of Bansal and Lehmann (1997)

Here I consider a bound on the logarithm of the SDF. By an application of Jensen's inequality, we get

$$\begin{aligned} 0 = \log(1) = \log \mathbb{E}\left[MR\right] &\geq \mathbb{E}\left[\log M\right] + \mathbb{E}\left[\log R\right] \\ \implies -\mathbb{E}\left[\log M\right] &\geq \mathbb{E}\left[\log R\right]. \end{aligned}$$

This bound, together with its asset pricing implications, is analyzed in detail by Bansal and Lehmann (1997). It is known to bind for the market portfolio in a representative agent model with log utility. Applying a log transformation to (D.1), we obtain for any $\tau \in (0,1)$

$$\log(\tau) = \log(R_f) + \log\left(\mathbb{E}\left[M\mathbb{1}\left(R \leq \widetilde{Q}_\tau\right)\right]\right).$$

Using Jensen's inequality and rearranging gives

$$-\mathbb{E}\left[\log\left(M\right)\right] \geq \log(R_f) + \mathbb{E}\left[\log\left(\mathbb{1}\left(R \leq \widetilde{Q}_\tau\right)\right)\right] - \log(\tau).$$

D.3 Bound of Liu (2021)

Liu (2021) develops a continuum of bounds that are based on different moments of the SDF. In particular

$$\mathbb{E}\left[M^s\right] \begin{cases} \leq \mathbb{E}\left[R^{-\frac{s}{1-s}}\right]^{1-s}, & \text{if } s \in (0,1). \\ \geq \mathbb{E}\left[R^{-\frac{s}{1-s}}\right]^{1-s}, & \text{if } s \in (-\infty, 0). \end{cases} \tag{D.2}$$

The proof, as in Liu (2021), follows from an application of the *reverse Hölder inequality*.[32] Equality occurs for the return which satisfies

$$\log M = -\frac{1}{1-s}\log R + \text{Constant}.$$

The quantile relation can only be used to obtain the upper bound part in (D.2), since the reverse Hölder inequality requires almost sure positivity of $\mathbb{1}(R \leq \widetilde{Q}_\tau)$ to prove

[32] The reverse Hölder inequality states that for any $p \in (1,\infty)$ and measure space (S, Σ, μ) that satisfies $\mu(S) > 0$. Then for all measurable real- or complex-valued functions f and g on S such that $g(s) \neq 0$ for μ-almost all $s \in S$, $\|fg\|_1 \geq \|f\|_{\frac{1}{p}} \|g\|_{\frac{-1}{p-1}}$.

the lower bound. For $p \in (1, \infty)$, apply the reverse Hölder inequality to the relation (D.1) to obtain

$$\tau = R_f \mathbb{E}\left[M \mathbb{1}\left(R \leq \widetilde{Q}_\tau\right)\right] \geq R_f \mathbb{E}\left[M^{\frac{-1}{p-1}}\right]^{1-p} \mathbb{E}\left[\mathbb{1}\left(R \leq \widetilde{Q}_\tau\right)^{\frac{1}{p}}\right]^p$$

Rearranging and using $s \coloneqq -\frac{1}{p-1} \in (-\infty, 0)$ yields

$$\mathbb{E}\left[M^s\right] \geq \left(\frac{\tau}{R_f}\right)^s \mathbb{E}\left[\mathbb{1}\left(R \leq \widetilde{Q}_\tau\right)\right]^{1-s}.$$

E Risk-adjustment in the data and in asset pricing models

In this Section, I analyze the approximation to the physical quantile function

$$Q_{t,\tau} \approx \widetilde{Q}_{t,\tau} + \frac{\mathrm{LB}_{t,\tau}}{\widetilde{f}_t(\widetilde{Q}_{t,\tau})} =: \widetilde{Q}_{t,\tau} + \mathrm{RA}_{t,\tau}.$$

E.1 Risk-adjustment term in the data

In the empirical application, I compute the risk-adjustment term, $\mathrm{RA}_{t,\tau} = \mathrm{LB}_{t,\tau}/\widetilde{f}_t(\widetilde{Q}_{t,\tau})$, for the 30, 60 and 90 day horizon. Table E1 contains summary statistics of $\mathrm{RA}_{t,\tau}$. The risk-adjustment term is right-skewed and is most significant for the 5 and 10% quantile. Moreover, over the 30 day horizon, it can spike up to 25% and averages to about 1% in the far left tail. In annual units, this average implies that the risk-neutral and physical quantile differ by 11%, when $\tau = 0.05$.

E.2 Robustness of the risk-adjustment term and risk-neutral quantile

The risk-adjustment term, $\mathrm{RA}_{t,\tau}$, tries to capture the difference between the physical and risk-neutral quantile in the left tail. What are some other measures that are available at a daily frequency and contain information about the quantile wedge? One candidate is the VIX index, which is defined as

$$\mathrm{VIX}^2 = \frac{2R_{f,t\to N}}{\Delta T}\left[\int_0^{F_t} \frac{1}{K^2}\mathrm{Put}_t(K)\,\mathrm{d}K + \int_{F_t}^{\infty} \frac{1}{K^2}\mathrm{Call}_t(K)\,\mathrm{d}K\right],$$

where ΔT is the time to expiration, F_t is the forward price on the S&P500, and $\mathrm{Put}_t(K)$ (resp. $\mathrm{Call}_t(K)$) is the put (resp. call) option price on the S&P 500 with

Table E1: **Summary statistics risk-adjustment term**

	Horizon (in days)	Mean	Median	Std. dev.	Min	Max
$\tau = 0.05$	30	0.92	0.63	1.07	0.08	24.38
	60	1.81	1.31	1.67	0.1	19.23
	90	2.65	2.02	2.02	0.02	18.63
$\tau = 0.1$	30	0.7	0.45	0.87	0.06	12.22
	60	1.71	1.19	1.66	0.25	19.89
	90	2.86	2.12	2.32	0.04	24.47
$\tau = 0.2$	30	0.47	0.25	0.74	0.04	10.93
	60	1.14	0.69	1.5	0.12	23.57
	90	1.97	1.22	2.33	0.26	28.92

Note: This table reports summary statistics of the risk-adjustment term, $\text{RA}_{t,\tau} = \text{LB}_{t,\tau}/\widetilde{f}_t(\widetilde{Q}_{t,\tau})$, in (6.16) at different time horizons and different quantile levels over the sample period 2003-2021. All statistics are in percentage point.

strike K. Martin (2017) shows that VIX measures risk-neutral entropy

$$\text{VIX}^2 = \frac{2}{\Delta T}\widetilde{L}_t\left(\frac{R_{m,t\to N}}{R_{f,t\to N}}\right),$$

where entropy is defined as $\widetilde{L}_t(X) \coloneqq \log \widetilde{\mathbb{E}}_t[X] - \widetilde{\mathbb{E}}_t[\log X]$. Entropy, just like variance, is a measure of spread in the distribution. However, entropy places more weight on left tail events than variance, since entropy places more weight on out-of-the money puts. As such, VIX is a good candidate to explain potential differences between $Q_{t,\tau}$ and $\widetilde{Q}_{t,\tau}$. Second, the Chicago Board Options Exchange provides daily data on VIX for the 30 day horizon.

Table E2 shows the result of the quantile regression

$$Q_{t,\tau}(R_{m,t\to N}) - \widetilde{Q}_{t,\tau}(R_{m,t\to N}) = \beta_0(\tau) + \beta_1(\tau)\text{RA}_{t,\tau} + \beta_{\text{VIX}}(\tau)\text{VIX}. \tag{E.1}$$

We see that β_{VIX} is marginally significant in the left tail. In contrast, $\beta_1(\tau)$ is even more significant compared to Table 4. Furthermore, the explanatory power of the model that only includes VIX is lower compared to the model that only includes $\text{RA}_{t,\tau}$ (Table 4).

As a second robustness check, I consider how well the direct quantile forecast, $\widehat{Q}_{t,\tau} = \widetilde{Q}_{t,\tau} + \text{RA}_{t,\tau}$, compares to the VIX forecast. Since $\widehat{Q}_{t,\tau}$ does not require any parameter estimation, this exercise is a measure of out-of-sample performance. However, VIX does not directly measure $Q_{t,\tau}$ and hence I use an expanding window to

Table E2: **Quantile regression lower bound and VIX**

	$\widehat{\beta}_0(\tau)$	$\widehat{\beta}_1(\tau)$	$\widehat{\beta}_{\text{VIX}}(\tau)$	$R^1(\tau)[\%]$	$R^1(\tau)[\%]$ (VIX only)
$\tau = 0.05$	-0.20 (2.021)	10.09 (0.345)	-0.30 (0.143)	6.34	5.51
$\tau = 0.1$	-0.35 (1.515)	5.06 (0.310)	-0.22 (0.100)	3.41	2.84
$\tau = 0.2$	-0.28 (1.112)	3.62 (0.265)	-0.25 (0.079)	0.61	0.18

Note: This table reports the QR estimates of (E.1) over the 30-day horizon. The sample period is 2003-2021, standard errors are shown in parentheses and calculated using SETBB with a block length of 5 times the forecast horizon. $R^1(\tau)$ denotes the goodness-of-fit measure (3.5). The last column denotes the goodness-of-fit in the model that only uses VIX as covariate. The standard error and point estimate of β_0 is multiplied by 100 for readability.

obtain the VIX benchmark: $\widehat{Q}^{\text{VIX}}_{t,\tau} := \widehat{\beta}_0(\tau) + \widehat{\beta}_1(\tau)\text{VIX}_t$. Finally, I use the following out-of-sample metric to compare both forecasts

$$R^1_{oos}(\tau) = 1 - \sum_{t=500}^{T} \rho_\tau(R_{m,t\to N} - \widehat{Q}_{t,\tau}) / \sum_{t=500}^{T} \rho_\tau(R_{m,t\to N} - \widehat{Q}^{\text{VIX}}_{t,\tau}).$$

Notice that $R^1_{oos}(\tau) > 0$, if $\widehat{Q}_{t,\tau}$ attains a lower error than $\widehat{Q}^{\text{VIX}}_{t,\tau}$. This exercise is more ambitious, since $\widehat{Q}^{\text{VIX}}_{t,\tau}$ makes use of in-sample information. Nonetheless, Figure E2 shows that $\widehat{Q}_{t,\tau}$ outperforms the VIX predictor at all quantile levels.

Figure E3 performs a similar exercise in the right tail, but instead of using $\widehat{Q}_{t,\tau}$, I use $\widetilde{Q}_{t,\tau}$, since Table 1 shows that the risk-neutral quantile is a good approximation to $Q_{t,\tau}$ in the right tail. We see that $\widetilde{Q}_{t,\tau}$ outperforms $\widehat{Q}^{\text{VIX}}_{t,\tau}$ at all quantile levels. Hence, the risk-neutral approximation in the right tail is more accurate than using the in-sample VIX measure.

E.3 Lower bound in Black-Scholes model

This section illustrates the accuracy of the quantile approximation in (6.12) in a discretized version of the Black-Scholes model with time varying parameters. Specifically, I assume the following DGP

$$R_{m,t\to N} = \exp\left((\mu_t - \frac{1}{2}\sigma_t^2)N + \sigma_t\sqrt{N}Z_{t+N}\right), \quad Z_{t+N} \sim N(0,1) \tag{E.2}$$
$$\sigma_t \sim \textbf{Unif}[0.05, 0.35]$$
$$\mu_t \sim \textbf{Unif}[-0.02, 0.2]\,.$$

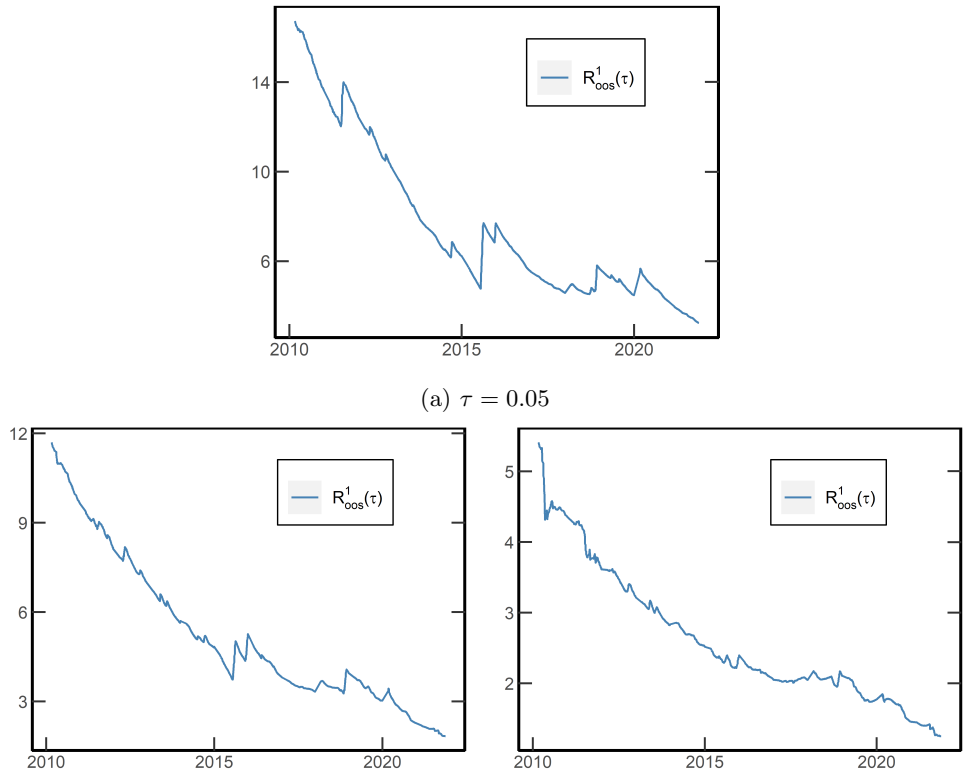

(a) $\tau = 0.05$

(b) $\tau = 0.1$

(c) $\tau = 0.2$

Figure E2: **Out-of-sample forecast using risk-adjusted quantile with VIX benchmark**. This figure shows the cumulative out-of sample $R^1(\tau)$, defined as $R^1_{oos}(\tau) = 1 - \sum_{t=500}^{T} \rho_\tau(R_{m,t\to N} - \widehat{Q}_{t,\tau}) / \sum_{t=500}^{T} \rho_\tau(R_{m,t\to N} - \widehat{Q}^{\text{VIX}}_{t,\tau})$, where $\widehat{Q}_{t,\tau} = \widetilde{Q}_{t,\tau} + \text{RA}_{t,\tau}$, $\widehat{Q}^{\text{VIX}}_{t,\tau} = \widehat{\beta}_0(\tau) + \widehat{\beta}_1(\tau) \cdot \text{VIX}_t$, and $\widehat{\beta}_0(\tau), \widehat{\beta}_1(\tau)$ are the regression estimates from a quantile regression of $R_{m,t\to N}$ on VIX_t, using data only up to time t. The horizon is 30 days and the QR estimates are dynamically updated using an expanding window over the period 2003–2021. The initial sample uses 500 observations.

The return distribution under risk-neutral dynamics is given by

$$\widetilde{R}_{m,t\to N} = \exp\left((r_t - \frac{1}{2}\sigma_t^2)N + \sigma_t\sqrt{N}Z_{t+N}\right) \tag{E.3}$$

$$r_t \sim \textbf{Unif}\,[0, 0.03]\,. \tag{E.4}$$

Finally, assume that all parameters are IID over time and that options are priced according to the Black-Scholes formula, conditional on time t. In this setup, it is fruitless to use historical data to predict future quantiles, since parameters change unpredictably over time. We use $N = 30$ to mimic the monthly application in this paper. It is assumed that the risk-neutral quantile function is known at the start of period t, as it is in the real world, by the result of Breeden and Litzenberger (1978). I use the risk-neutral quantile function to calculate $\text{LB}_{t,\tau}$ at time t. Then, following

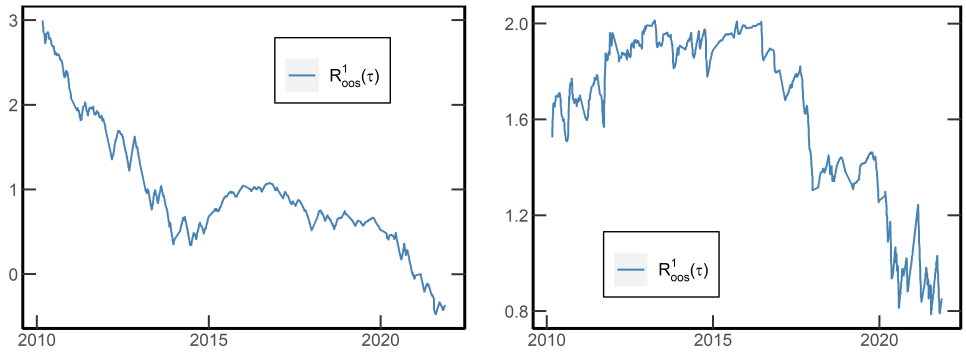

(a) $\tau = 0.5$

(b) $\tau = 0.8$

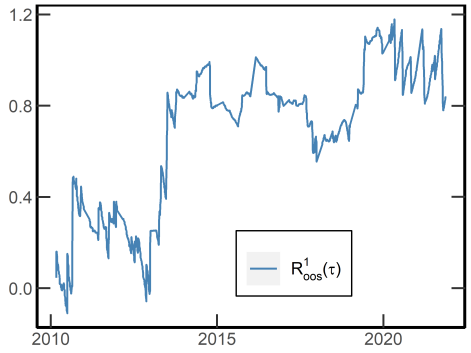

(c) $\tau = 0.9$

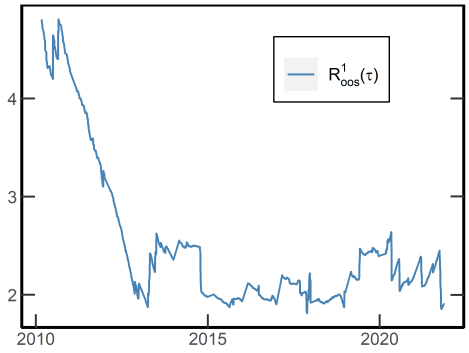

(d) $\tau = 0.95$

Figure E3: **Out-of-sample forecast using risk-neutral quantile with VIX benchmark.** This figure shows the cumulative out-of sample $R^1(\tau)$, defined as $R^1_{oos}(\tau) = 1 - \sum_{t=500}^{T} \rho_\tau(R_{m,t\to N} - \widetilde{Q}_{t,\tau}) / \sum_{t=500}^{T} \rho_\tau(R_{m,t\to N} - \widehat{Q}^{\text{VIX}}_{t,\tau})$, where $\widehat{Q}^{\text{VIX}}_{t,\tau} = \widehat{\beta}_0(\tau) + \widehat{\beta}_1(\tau) \cdot \text{VIX}_t$, and $\widehat{\beta}_0(\tau), \widehat{\beta}_1(\tau)$ are the regression estimates from a quantile regression of $R_{m,t\to N}$ on VIX_t, using data only up to time t. The horizon is 30 days and the QR estimates are dynamically updated using an expanding window over the period 2003–2021. The initial sample uses 500 observations.

the approximation in (6.12), the physical quantile function is estimated by

$$\widehat{Q}_{t,\tau} = \widetilde{Q}_{t,\tau} + \text{RA}_{t,\tau}. \tag{E.5}$$

We take 3,000 return observations that are generated according to (E.2). This exercise is repeated 1,000 times. To assess the accuracy of the approximation in (E.5), I use several metrics. For every sample, I estimate a quantile regression of the form

$$Q_\tau(R_{t+1}) = \beta_0(\tau) + \beta_1(\tau)\widehat{Q}_{t,\tau},$$

where $\widehat{Q}_{t,\tau}$ comes from (E.5). The first two columns in Table E3 report the average values of the QR estimates across the 1,000 simulations. The means are rather close to 0 and 1 respectively for all quantiles. If (6.4) is a good approximation, one expects $Q_{t,\tau} > \widehat{Q}_{t,\tau}$, since $\text{LB}_{t,\tau} \leq \tau - F_t(\widetilde{Q}_{t,\tau})$. The third column in Table

E3 shows this happens for the majority of samples. The fourth column shows the correlation between $Q_{t,\tau}$ and $\widehat{Q}_{t,\tau}$, which is very close to one, and corroborates the view that the approximation is quite accurate. Columns four and five document the percentage of non rejection of H_0, which is indeed quite high. The last column considers non rejection of the joint null hypothesis, which is also high except for the $\tau = 0.1$ quantile. Overall, Table E3 suggests that (E.5) is a highly accurate predictor of the physical quantile function.

Table E3: Simulation results

	$\mathbb{E}\widehat{\beta}_0(\tau)$	$\mathbb{E}\widehat{\beta}_1(\tau)$	$Q > \widehat{Q}$	$\rho(Q, \widehat{Q})$	$\widehat{\beta}_0(\tau) = 0$	$\widehat{\beta}_1(\tau) = 1$	$[\widehat{\beta}_0(\tau), \widehat{\beta}_1(\tau)] = [0, 1]$
$\tau = 0.01$	0.01	0.99	0.85	1	0.94	0.96	0.8
$\tau = 0.05$	-0.03	1.04	0.69	0.99	0.9	0.89	0.66
$\tau = 0.1$	-0.06	1.07	0.64	0.99	0.78	0.76	0.47

Note: $\mathbb{E}\widehat{\beta}_0(\tau)$ denotes the average QR estimate of $\widehat{\beta}_0(\tau)$ and likewise $\mathbb{E}\widehat{\beta}_0(\tau)$ shows it for $\widehat{\beta}_1(\tau)$. $Q > \widehat{Q}$ shows the fraction of times the true physical quantile is larger than our predicted quantile. Columns $H_0 : \widehat{\beta}_0(\tau) = 0$ and $H_0 : \widehat{\beta}_1(\tau) = 1$ report the fraction of times the individual null hypotheses $\beta_0(\tau) = 0, \beta_1(\tau) = 1$ are not rejected. The last column reports the fraction of times the joint null hypothesis is not rejected.

Example E.1. I illustrate the approximation (6.4) in the Black-Scholes model with fixed parameters: $N = 365$ (one year), $\mu = 0.08, r = 0.02, \sigma = 0.2$.[33] We can explicitly calculate $F^{-1}, \widetilde{F}^{-1}$ and $\widetilde{f}$ owing to the lognormal assumption. Figure E4 shows the risk-neutral quantile function, the approximation (6.4) and the true physical quantile function. Observe that the approximation (6.4) is very accurate in this case.

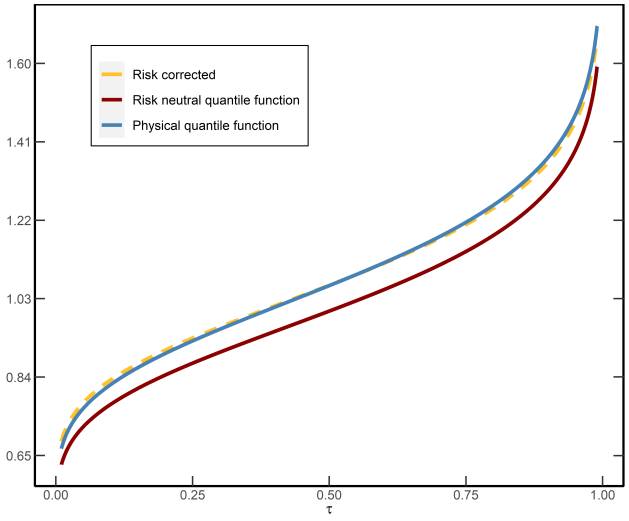

Figure E4: Illustration of quantile approximation (E.5) in the Black-Scholes model.

[33] For illustrative purposes, I use $\lambda = 1$, instead of $\lambda = 1/12$, otherwise the physical quantile function and its approximation are indistinguishable.

E.4 Bias in quantile regression

In the empirical application, we have to estimate $\widetilde{Q}_{t,\tau}, \widetilde{f}(\cdot)$ and $\text{LB}_{t,\tau}$. Therefore, the estimated coefficients in the quantile regression are biased, due to measurement error in the covariate. I present simulation evidence which shows that the bias is small in finite samples.

The setup is as follows. We simulate returns according to model (E.2) and assume that options are priced according to the Black and Scholes (1973) formula at the start of period t. We want to calculate the risk-adjustment term for a maturity of 90 days. As in the empirical application, I assume that options with an exact 90 day maturity are not available, but instead we observe options with maturity 85 and 97 days. I generate a total of 1,000 options every time period with maturities randomly sampled from 85 and 97 days.[34] These numbers are roughly consistent with the latter part of our empirical sample. The procedure is repeated for a total of 1,000 time periods. For the entire sample, I compare the estimated and analytical risk-adjustment term, which respectively are given by

$$\begin{aligned}
\text{RA}^e_{t,\tau} &:= \widehat{\widetilde{Q}}_{t,\tau} + \frac{\widehat{\text{LB}_{t,\tau}}}{\widehat{\widetilde{f}_t(\widetilde{Q}_{t,\tau})}} \\
\text{RA}^a_{t,\tau} &:= \widetilde{Q}_{t,\tau} + \frac{\text{LB}_{t,\tau}}{\widetilde{f}_t(\widetilde{Q}_{t,\tau})}.
\end{aligned}$$

The hats in $\text{RA}^e_{t,\tau}$ signify that the risk-neutral quantile, PDF and lower bound are estimated from the available options at time t, using the procedure in Appendix B.2. The terms in $\text{RA}^a_{t,\tau}$ are obtained from the known analytical expression of the risk-neutral distribution (recall (E.3)). I then use QR to estimate the models

$$\begin{aligned}
Q(R_{t+1}) &= \widehat{\beta}_0(\tau) + \widehat{\beta}_{1,e}(\tau)\text{RA}^e_{t,\tau} \\
Q(R_{t+1}) &= \widehat{\beta}_0(\tau) + \widehat{\beta}_{1,a}(\tau)\text{RA}^a_{t,\tau}.
\end{aligned}$$

I use the ratio $\widehat{\beta}_{1,e}/\widehat{\beta}_{1,a}$ to measure the relative bias in the sample. This is repeated 500 times to get a distribution of the relative bias. Figure E5 shows boxplots of the bias for several quantiles. We see that the relative bias is very small and centered around 1. Hence, the error in measurement problem resulting from estimating the risk-adjustment term is limited.

[34] So on average there will 500 options with maturity 85 days and 500 with maturity 97 days.

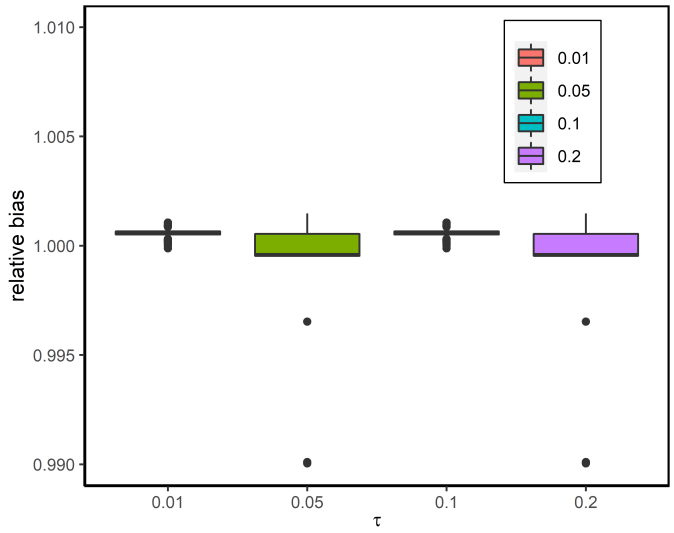

Figure E5: **Bias in QR resulting from measurement error.**